



- How unstable was the environment during the Penultimate
- 2 Glacial in the South-Western Mediterranean? Vegetation,
- 3 climate and human dynamics during MIS 6.
- 5 Liz Charton<sup>1,2</sup>, Nathalie Combourieu-Nebout<sup>1</sup>, Adele Bertini<sup>2</sup>, Odile Peyron<sup>3</sup>, Mary Robles<sup>3</sup>,
- 6 Vincent **Lebreton**<sup>1</sup>, Marie-Hélène **Moncel** <sup>1</sup>.
- 7 1: UMR 7194 HNHP- « Histoire Naturelle des Humanités Préhistorique », MNHN / CNRS / UPVD, Paris, France.
- 8 <u>liz.charton@mnhn.fr</u>
- 9 2 : Dipartimento di Scienze della Terra, Università degli Studi di Firenze, Florence, Italy.
- 3: UMR 5554, ISEM-Institut des Sciences de l'Evolution de Montpellier, CNRS, Université de Montpellier,
- 11 Montpellier, France.

### **Abstract**

13 14 15

> 16 17

> 18 19

20

21 22

23 24

25

26

27

28 29

30

31 32

33

34

35 36

37

12

4

The impact of rapid climate variability on Neanderthal population in Europe during the Last Glacial (Marine Isotope Stages 4-2), including Dansgaard-Oeschger cycles and Heinrich events, has been the subject of a long-standing debate. However, few studies have focused on the nature and impact of such rapid variations on human population during earlier periods. A growing number of high-resolution paleoclimatic archives supports the persistence of rapid oscillations during the penultimate glaciation (MIS 6), and the close response of Mediterranean ecosystems to these. Still, few palynological sequences in the Mediterranean region offer sufficient resolution to document vegetation dynamics during this time. Pollen records are especially lacking in the western Mediterranean, a key region to understand the connection between North Atlantic and Mediterranean climatic influences. This region is also traditionally considered a climatic refugium for human population during unfavourable periods. We provide new palynological data covering MIS 6 from the long and continuous marine record of ODP 976 in the Alboran Sea. A total of 200 samples, spanning the interval from 196 to 127 ka Before Present (BP), reveal both long-term trends and rapid fluctuations in regional vegetation composition. A multi-method approach, including modern analogues, regression, and machine learning approaches, was applied to ODP 976 pollen assemblages to reconstruct the annual/seasonal temperatures and precipitation. Results show that three phases can be identified. The first phase (187-166 ka BP) is characterized by significant oscillations of temperate trees and rather cool and humid conditions during early MIS 6, coincident with a sapropel layer deposition in both the western and eastern Mediterranean. In the second phase (165-144 ka BP), arid herbaceous vegetation is dominant, marking the main imprint of glacial maxima conditions and reduced climate variability. The third phase (144-129 ka BP) is marked by the development of Ericaceae and increased annual precipitations. At the end of MIS 6



39

40

41

42

43

44

45

46

47

48

49

52

53

54

55

56

57

58

59

60 61

62 63

64

65

66

67

68

69

70 71

72

73



glaciation, an strong cooling and intense episode of steppe and semi-desert expansion is identified as Heinrich Stadial 11 (135-129 ka BP), marking a distinct pattern for Termination II in the Western Mediterranean. Rapid oscillations appear like a pervasive feature of the Penultimate glacial in the SW Mediterranean, though they present reduced amplitude and frequency compared to the Last Glacial. A synthesis of human occupation shows that a mosaic of traditional (Mode 2) and innovative (Mode 3) technological features is observed. Although the data are scarce, Neanderthal seems to have continuously inhabited Western Mediterranean regions across the penultimate glacial. The severe climate conditions during Heinrich Stadial 11 (~133-129 ka BP) might have played a role in the apparent population contraction at the end of MIS 6, and perhaps also in the definitive abandonment of Lower Palaeolithic industries.

## 1. Introduction

5051 Rapid climate oscillations

Rapid climate oscillations occurred during the last Glacial period (Marine Isotope Stages "MIS" 4-2). Dansgaard-Oeschger (DO) cycles have been well identified in ice-core records (Bond et al., 1999; Dansgaard et al., 1993; Johnsen et al., 1992; Rasmussen et al., 2014) and recognized in Atlantic sedimentary cores (e.g. Bond et al., 1993, 1997; Roucoux et al., 2005; Sánchez Goñi et al., 2002; Shackleton et al., 2000, Zumaque et al., 2025). Short periods of intense cold named Heinrich Stadials (HS) and linked with intense iceberg discharges were also evidenced in Atlantic sediments (Bond et al., 1992; Heinrich, 1988; Hemming, 2004; Rasmussen et al., 2003; Ruddiman, 1977; Shackleton et al., 2004). These climate oscillations reflect major changes at global scale in the oceanic circulation and the Atlantic Meridional Overturning Circulation (AMOC), that are important features particularly during glacial terminations (Barker and Knorr, 2021). The Mediterranean region has been very sensitive to the rapid climate oscillations of MIS 5 to MIS 1, with changes recorded in both marine and continental environments (Cacho et al., 1999, 2006; Combourieu-Nebout et al., 2002, 2009; Fletcher et al., 2010; Martrat et al., 2007; Penaud et al., 2016; Sánchez Goñi et al., 2002, 2022). Major cooling events also occurred during the last interglacial (MIS 5) and the penultimate deglaciation (e.g. Chapman & Shackleton, 1999; Oppo et al., 2001); however, during MIS 6, these events are less documented than MIS 4-2.

The Penultimate glacial (MIS 6), took place between ~185 and 130 ka BP and presented a different ice-sheet and global climate configuration compared to the last glacial (MIS 4-2). It is considered among the coldest glacial periods of the past 800 ka BP (Masson-Delmotte et al., 2010), characterized by larger European Ice-Sheet and smaller Laurentide ice-sheet extension (Colleoni et al., 2016; Ehlers et al., 2018; Ehlers & Gibbard, 2007; Rohling et al., 2017). In Europe, it corresponds to the Riss glaciation in the Alpine area, and to the late Saalian

https://doi.org/10.5194/egusphere-2025-5024 Preprint. Discussion started: 21 October 2025 © Author(s) 2025. CC BY 4.0 License.



75

77

78 79

81 82

83 84

85

87

89

91

92

93

94

95

96 97

98

99

100

101

102

103 104

105

106

107

108



74 glaciation complex in northern and central Europe, with two major ice-sheet advances identified in Germany: the Drenthe advance (~170-155 ka BP) characterized by the maximum ice extent in Europe, and the less extensive Warthe advance during the younger stage of MIS 76 6 (Ehlers et al., 2011). The exact chronology of the Penultimate Glacial Maximum (i.e. the maximum extension of the northern hemisphere ice-sheet) is still not well constrained (Svendsen et al., 2004), but is usually considered around 140 ka BP (Colleoni et al., 2016). Five marine isotopic substages were identified from MIS 6e to 6a, reflecting variations of global 80 sea temperatures: three cold substages (6e: ~180 ka BP, 6c: ~160 ka BP, 6a: ~136 ka BP) with increasing cold intensity, and two warm substages (6d: ~170 ka BP and 6b: ~149 ka BP) (Railsback et al., 2015). Different speleothem records revealed that MIS 6 glaciation in Europe, including the Mediterranean region, was characterized by wetter conditions in comparison with the last glacial (Ayalon et al., 2002; Koltai et al., 2017; Nehme et al., 2018; Regattieri et al., 86 2014). Furthermore, various studies highlighted the apparent higher stability of the Laurentide ice-sheets during the penultimate glacial, leading to the absence of typical "Heinrich layers" in 88 the North Atlantic sediments, with the exception of the large event recorded at the MIS 6 to MIS 5 transition and known as HS11 (~135-129 ka BP) (de Abreu et al., 2003; McCarron et al., 2021; McManus et al., 1999; Obrochta et al., 2014; Ovsepyan and Murdmaa, 2017; 90 Shackleton et al., 2003).

Human Palaeolithic groups in Europe were likely affected by rapid climate changes (Bradtmöller et al., 2012; Dennell et al., 2011; Raia et al., 2020; Willis et al., 2004). The South-Western Mediterranean probably played a major role as one of the climate refugia area around the Mediterranean Basin during the most unfavourable climatic periods, permitting the persistence of "source" population able to recolonize the northernmost areas during more favourable periods (Bailey et al., 2008; Bicho & Carvalho, 2022). Many studies focused on the potential impact of abrupt environmental changes on Neanderthal populations, especially those associated with Heinrich Stadials during MIS 3 (e.g. Charton et al., 2025; D'Errico & Sánchez Goñi, 2003; Finlayson & Carrión, 2007; Melchionna et al., 2018). During the previous climatic cycles of the Middle Pleistocene, when Early to Middle Palaeolithic cultures developed, repeated climate instability has been brought forward as an explanation for the large variability in the lithic production (Dennell et al., 2011; Foerster et al., 2022; Sánchez-Yustos and Diez-Martín, 2015), and the non-linearity of the biological processes linked with Neanderthal evolution (Bermúdez de Castro & Martinón-Torres, 2013; Hublin, 2009). Still, the short and long-term resilience of human populations in a globally unstable environment, as during the MIS 6 glacial, is poorly understood and partially hindered by our limited knowledge of fast millennial-scale climate oscillations in older glaciations prior to MIS 4-2.



110

111

112

113

114

115

116117

118

119

120121

122

123

124

125

126

127

128 129

130131

132

133134

135

136

137

138

139

140

141



While the Greenland ice does not provide an adequate record for periods older than 123 ka BP (Chappellaz et al., 1997), the description of a precise stratigraphy of climate events at sub millennial scale for the previous glacial/interglacial cycles remains complex, and relies on the Antarctic isotope record (Bazin et al., 2013; Jouzel et al., 2007), the study of marine sediments (de Abreu et al., 2003; Lisiecki & Raymo, 2005; Margari et al., 2010, 2014; McManus et al., 1999; Obrochta et al., 2014) and high-resolution continental archives such as speleothems (Burns et al., 2019; Held et al., 2024; Hodge et al., 2008; Wainer et al., 2013; Wang et al., 2018; Wang et al., 2001). Benthic and planktonic isotopic ratios together with Sea Surface Temperatures (SSTs) reconstructions in the North Atlantic and the Western Mediterranean showcased the persistence of D-O-like events and interhemispheric bipolar see-saw heat transport during MIS 6, in addition to important reorganization of the water circulation during sapropel S6 deposition ~175 ka BP (Margari et al., 2010, 2014; Martrat et al., 2004, 2007, 2014; Rousseau et al., 2020; Sierro & Andersen, 2022). Nevertheless, MIS 6 is much less well documented than the last glacial in Mediterranean Europe. Few palynological sequences are available to document the vegetation changes across this interval (Camuera et al., 2019, 2022; Follieri et al., 1988; Margari et al., 2010; Okuda et al., 2001; Roucoux et al., 2011; Sadori et al., 2016; Sinopoli et al., 2019; Tzedakis et al., 2006; Wilson et al., 2021). Among them, only one in SW Europe provides sufficient resolution to document high-frequency changes: the deep-sea core MD01-2444 (Margari et al., 2010, 2014). While D-O like events impacting the vegetation have been identified in this record especially during the lower MIS 6, the core is located out of the Mediterranean Sea along the Portuguese margin in the Atlantic Ocean. Therefore, questions remain open concerning the impact of such events on the Western Mediterranean region, considered a Pleistocene refugium for human populations.

To adress this gap, our study presents high-resolution pollen data and quantitative climate reconstructions from ODP site 976, located in the southwestern Mediterranean, focusing on MIS 6. We aim to (i) reconstruct the vegetation and climate changes in the SW Mediterranean during the penultimate glacial, (ii) identify abrupt climatic changes including potential Heinrich-like and D-O like events and connect them with other Atlantic and Mediterranean paleoenvironmental records, (iii) compare the nature of millennial-scale climate and vegetation dynamics during the last glacial period (MIS 4-2) and the penultimate glacial (MIS 6) using a single, continuous pollen record and (iv) explore the potential impact of these climatic changes for Early Middle Palaeolithic human groups, with particular attention to the presence of climate refugia during the most extreme glacial phases.

## 2. Study site





Ocean Drilling Program (ODP) Site 976 (36°12 N, 4°18W, 1108 m depth) core was retrieved in 1995 in the Alboran Sea (Zahn et al., 1999). The site is located about 110 km east of the Gibraltar Strait, 70 km south of the Spanish coast, and 100 km north of Morocco (Fig. 1).

The Alboran Sea is the westernmost extensional basin of the Mediterranean Sea, bordered to the north by the Betic Cordillera and to the south by the Moroccan Rif mountains. Oceanic currents result from the water masses exchanges between the Atlantic Ocean and the Mediterranean Sea through the Gibraltar Strait. The surface currents are governed by the inflow of low-salinity Atlantic waters (Atlantic Jet) forming two anticyclonic gyres named Western and Eastern Alboran Gyres (WAG and EAG) (Renault et al., 2012) (Fig. 1). The Mediterranean high-salinity water masses flow out in the Atlantic basin through the intermediate depth currents.

The modern climate in the Alboran Sea region is typically Mediterranean, defined by long, hot, dry summers and mild and cool winters (Lionello et al., 2006; Pons and Quézel, 1998). Atlantic westerlies dominate during winter, while subtropical high pressure masses generate intense drought during summer (Sumner et al., 2001). The current vegetation distribution on the Alboran borderlands follows a strong altitudinal climatic gradient: dry steppe elements such as *Artemisia* and *Lygeum* grow in the most arid lowlands along the coast, sclerophyllous evergreen taxa, including *Quercus ilex*, *Olea* and *Pistacia* are the main representatives of the thermo-to meso-Mediterranean belts, while temperate vegetation with deciduous trees constitutes the overlying supra-Mediterranean belt (Quézel, 2000). Finally, coniferous forests of *Abies*, *Pinus* and *Picea* grow in the oro-Mediterranean belt (above approximately 1200 m), with the presence of *Cedrus* in altitudinal vegetation of the Moroccan Rif mountains.

The main sedimentation processes in the area originate from the strong erosion in the Betic Cordillera (Alonso et al., 1999; Liquete et al., 2005; Lobo et al., 2006) and the material transported by the Atlantic waters (Auffret et al., 1974), although a significant but unknown proportion of particles including pollen was transported by African winds as evidenced by the presence of Saharan clay particles and *Cedrus* pollen across the Pleistocene (Bout-Roumazeilles et al., 2007; Jiménez-Moreno et al., 2020; Magri and Parra, 2002). Therefore, the pollen assemblage is interpreted as reflecting the regional vegetation of the southern Iberian Peninsula, with smaller but variable contribution from Northern Africa. Previous studies have shown that the Alboran Sea palynological record displays close similarities with the Padul record in SE Spain (Camuera et al., 2019), indicating that ODP 976 is a valid archive to reconstruct the southern Iberian Peninsula vegetation changes (Fletcher & Sánchez Goñi, 2008; Charton et al., 2025).



180

181

182

183

184

185

186



Two Organic-Rich Layers (ORLs) were identified in ODP 976 core during the MIS 6 interval, bed 607 (50.43-49.93 m), and bed 606 (41.6-40.4 m) (Murat, 1999). The ages were recalculated based on the updated age model for MIS 6 presented here, giving 178.07-174.53 ka BP for bed 607, and 132.64-129.16 ka BP for bed 606. With a Total Organic Carbon (TOC) of 1.18% and 1.85% respectively, these layers have been described as "ghost sapropels", as they present a lower organic matter content than the Eastern Mediterranean sapropels (Rogerson et al., 2008). Their relevance for hydrological and climatic inferences in the Alboran Sea will be discussed in the light of the vegetation dynamics.

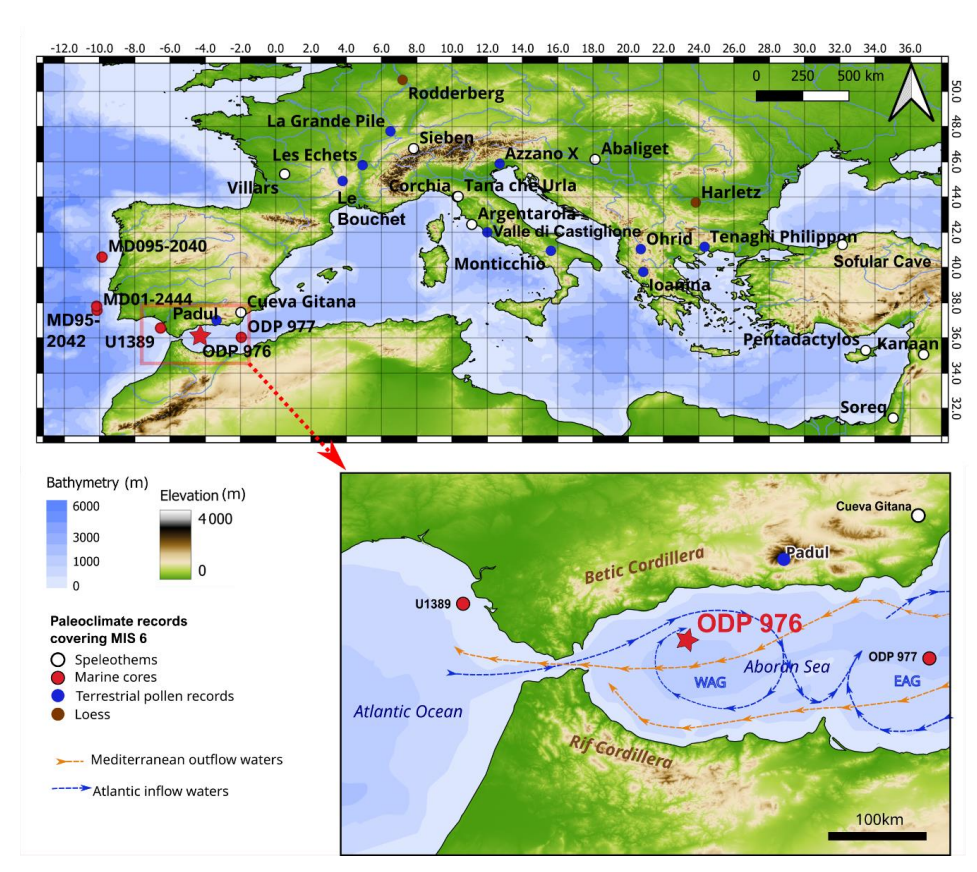


Fig. 1: Map showing the location of ODP 976 core together with other paleoenvironmental and paleoclimate records covering part or all of MIS 6, as discussed in the text.

188 3. Methods 189

187

190

Age Model





The age model for the study interval uses three previously published tie-points between ODP 976 Mg/Ca-derived SST (Jiménez-Amat and Zahn, 2015) and the speleothem temperature record from Dongge cave in China (Kelly et al., 2006). For the lower interval, the low resolution of planktonic isotopic data available for ODP 976 did not allow direct orbital or temperature calibration (von Grafenstein et al., 1999). Instead, we chose to align the higher-resolution pollen record produced in this study with the one from MD01-2444 core on the Portuguese margin (Margari et al., 2010, 2014; Tzedakis et al., 2018). Previous studies highlighted the strong similarities between pollen records on the Atlantic margin and the Alboran Sea during the last glacial period (Fletcher et al., 2010; Fletcher & Sánchez Goñi, 2008; Sánchez Goñi et al., 2002), supporting this approach. MD01-2444 chronology is based on the alignment of benthic isotopic events with the Antarctic temperature record, on AICC2012 timescale (Jouzel et al., 2007; Margari et al., 2010; Shin et al., 2020). Five peaks of temperate forest in MD01-2444 were used as control-points for ODP 976 (Table 1). A linear regression was applied to obtain a continuous age for the study interval, spanning from 124 to 196.6 ka BP, with a mean resolution of about 350 years for the record (Fig. 2).

Event type	ODP 976 Depth (mcd)	Age (ka BP)	References
Dongge cave speleothem D3	40.25	128.73	Jiménez-Amat and Zahn, 2015; Kelly et al., 2006
Dongge cave speleothem D2	42.61	135.57	Jiménez-Amat and Zahn, 2015; Kelly et al., 2006
Dongge cave speleothem D1	44.14	142.09	Jiménez-Amat and Zahn, 2015; Kelly et al., 2006
Temperate pollen peak in MD01-2444	46.4	149.43	(Margari et al., 2010; Shin et al., 2020)
Temperate pollen peak in MD01-2444	48.5	160.00	(Margari et al., 2010; Shin et al., 2020)
Temperate pollen peak in MD01-2444	49.3	170.07	(Margari et al., 2010; Shin et al., 2020)
Temperate pollen peak in MD01-2444	50.48	178.42	(Margari et al., 2010; Shin et al., 2020)
Temperate pollen peak in MD01-2444	52.2	193.758	(Margari et al., 2010; Shin et al., 2020)

Table 1: list of control points used to calibrate the ODP 976 record for the MIS 6 interval. The tie-points on MD01-2444 temperate pollen curve are on AICC2012 timescale.





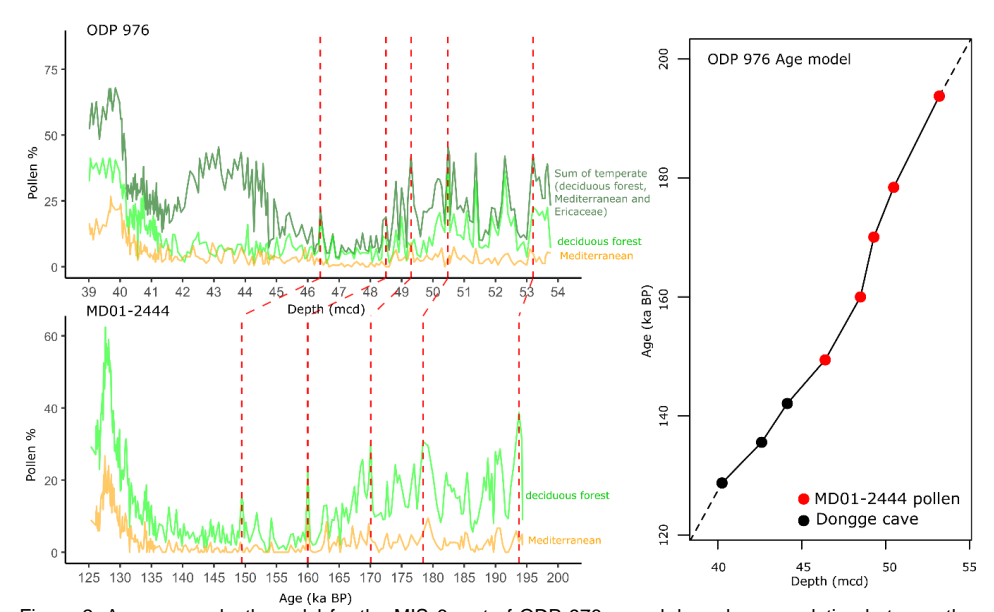


Figure 2: Age versus depth model for the MIS 6 part of ODP 976 record, based on correlation between the Mg/Ca-based SST curve (Jiménez-Amat and Zahn, 2015) and the Dongge cave speleothem temperature record (Kelly et al., 2006) (black dots), and graphical correlation of the temperate pollen curve with the MD01-2444 palynological record (red dots and dotted lines) on AICC2012 timescale (Margari et al., 2010; Shin et al., 2020).

#### 3.2. Pollen analyses

Two hundred samples have been analysed here, between 40 and 54 m (mcd) depth. The sample processing followed the traditional steps used for pollen extraction (Faegri and Iversen, 1964) and previously applied to the ODP 976 core (Combourieu-Nebout et al., 2002; 2009; Sassoon et al., 2023, Charton et al., 2025). It included sample weighing between 5 and 10 g of sediments, a 150  $\mu$ m sieving for the retrieving of macrofossils and macroparticles, followed by 10% HCI, 40% HF, 20% HCI and a final 10  $\mu$ m sieving.

A minimum of 150 pollen grains were counted for each sample, excluding *Pinus* as it is usually overrepresented in marine sequences (e.g. Combourieu-Nebout et al., 2002; Fletcher et al., 2010; Mudie, 2011 and references therein), and represents often more than 50% of the total pollen sum along the study interval (see Fig. 3).

Ecological groups of pollen taxa were defined following previous studies of the ODP 976 record (Charton et al, 2025; Combourieu-Nebout et al., 2009; Sassoon et al., 2023). The percentage pollen diagram was constructed using the *rioja* R package (Juggins, 2023). Constrained Incremental Sum-of-Squares (CONISS) cluster analysis was applied for pollen zonation, using the *vegan* package on R (Oksanen et al., 2024).





## 3.3. Pollen-inferred climate reconstructions: a multi-method approach

231232

233234

235

236

237

238

239

240

241

242243

244245

246247

248

249

250

251

252

253

254

255256

257

258259

260

261262

263264

230

Four methods were applied to the ODP 976 record to reconstruct past climate changes during MIS 6. This is the first time this approach is used for the entire MIS 6 interval (Sinopoli et al., 2019). As already pointed out, the multi-method approach allows for a more accurate climate reconstruction (trends and rapid events) compared to the traditional single-method approach (Chevalier et al., 2020; Peyron et al., 2011, 2013; Salonen et al., 2019; Sassoon et al., 2025). It also allows to compare the reliability and biases of the different methods, which are based on different ecological principles and mathematical algorithms. Four methods were used in this study.

The Modern Analogue Technique (MAT) is the first "assemblage" method ever developed to estimate climate parameters based on pollen assemblages, and is still the most widely used (Guiot, 1990). It is based on the calculation of a dissimilarity index between the fossil samples and samples from a modern pollen dataset. The values of the closest modern analogues selected (here, 4) are averaged to reconstruct the climate parameters for each fossil sample. Weighted-Averaging Partial Least Squares (WA-PLS) (ter Braak and Juggins, 1993) is the second most widely used method, and is based on a different mathematical approach using non-linear regression. Assuming that taxa are most abundant where they find their optimum climatic conditions, WA-PLS models the plant/climate relationships from the modern calibration dataset, weighing the climatic values based on the pollen taxa percentage. These plant pollen abundance / climate transfer functions are then used to calculate the climate parameters of the fossil samples. The last two methods, Random Forest (RF) and Boosted Regression Trees (BRT), rely on a completely different approach using machine learning: they generate a large set of regression trees based on a randomised pollen dataset by bootstrapping (with pollen taxa selected randomly). Contrary to RF (Prasad et al., 2006), BRT (Salonen et al., 2012) assigns a higher probability to select samples that have not been selected before (boosting), increasing the performance of the model for elements that are less well predicted (Chevalier et al., 2020). The application of these machine learning methodologies in paleoclimatology is very promising, especially for BRT, and they have already been validated through different European and Mediterranean pollen records, for different time periods (Charton et al. 2025; D'Oliveira et al., 2023; Robles et al., 2022, 2023; Salonen et al., 2019; Sassoon et al., 2025).

The four methods were run on R using packages *Rioja* for MAT and WA-PLS (Juggins, 2024), *dismo* for BRT (Hijmans et al., 2023) and *randomForest* for RF (Liaw and Wiener, 2022).

We used the modern pollen dataset compiled by Peyron et al. (2013, 2017) and updated by Dugerdil et al. (2021) and Robles et al. (2023). Samples belonging to non-relevant biomes





for this study were excluded (Taiga, Tundra, Pioneer Forest, warm steppe and hot desert), resulting in 2373 samples for calibration dataset spanning across Eurasia and NW Africa.

Six climate variables were reconstructed: PANN (annual precipitations), TANN (annual temperatures), SUMMERPR (summer precipitations), WINTERPR (winter precipitations), MTWA (mean temperature of the warmest month) and MTCO (mean temperature of the coldest month). SUMMERPR and MTWA values were poorly reconstructed according to the accuracy indicators (Table 2). This is in agreement with previous studies showing the poor reliability of summer parameters (e.g. Camuera et al., 2022). Therefore, we chose to represent seasonal parameters as contrast values for a better visualization: TCON (temperature contrast) = MTCO - MTWA, and PCON (precipitation contrast) = WINTERPR – SUMMERPR.

For comparison with the present-day climate, and the calculation of anomalies, the modern values were extracted from ERA 5 reanalysis of the ECMWF (European Centre for Medium-Range Weather Forecasts), based on data assimilation into meteorological modelling from 1960 to 2022 (Hersbach et al., 2020). An averaged value of the climate parameters on a 400 km radius around the ODP 976 site was extracted, giving MAP = 478 mm, TANN = 16.78°C, MTCO = 13.78 °C, WINTERPR = 172 mm, TCON = -9.59, PCON = 141.5 mm (see Supplementary materials S1). These values for modern climate, averaged temporally and spatially, provide a better basis for understanding the nature of the climate signal extracted from a marine palynological sequence at a regional pluri-annual scale.

The reliability of the different methods and climate parameters reconstructed is evaluated with bootstrapping cross-validation through two indicators: the correlation coefficient between the variables (R<sup>2</sup>) and the root mean square error (RMSE).

#### Results

## 4.1. Pollen record

The pollen diagram shows the vegetation dynamics between 196.6 and 127.5 ka BP, spanning late MIS 7 to early MIS 5 (Fig. 3). Five pollen zones were separated by CONISS cluster analysis, with zone 4 being divided in three subzones (Table 2).





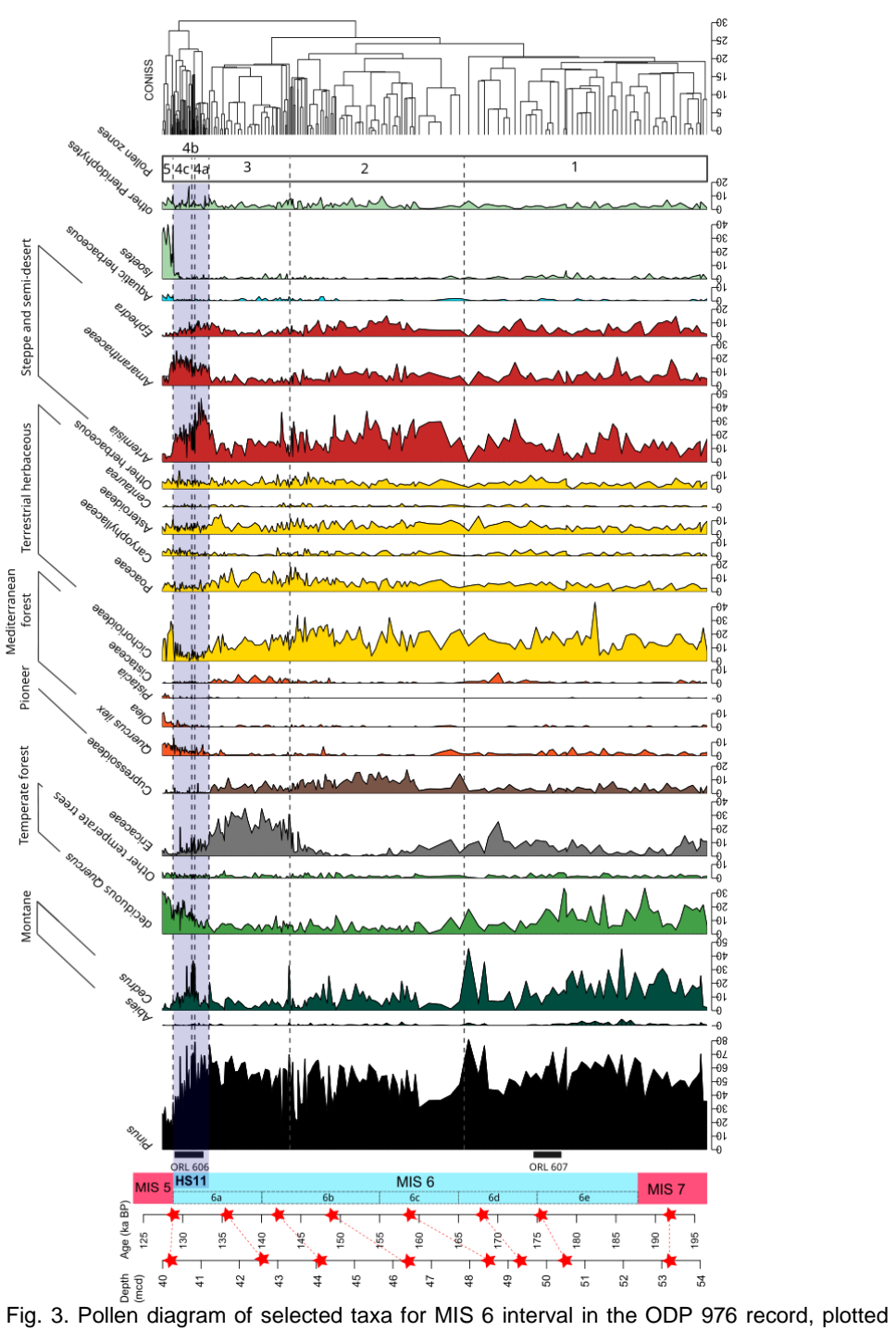


Fig. 3. Pollen diagram of selected taxa for MIS 6 interval in the ODP 976 record, plotted against age. Taxa are grouped by ecological groups (see Table 2). Red stars indicate control points used for the age calibration, and their correspondence with mcd (meters composite





depth) (see Table 1). The blue bar indicates Heinrich Stadial 11.ORL: Organic Rich Layers from ODP 976 (Murat, 1999).

293294

295

296297

298299

300

301

302

303

304

305

306 307

308 309

310

311

312

313314

Zone 1 most represented taxa are deciduous Quercus and Cedrus, with important abundance variability showing an unstable and rather cool and humid phase at the transition from MIS 7 to MIS 6e and 6d. Zone 2 displays the maximum expansion of steppe and semidesert vegetation together with other open vegetation taxa and Cupressoideae, characteristic of the vegetation maximum glacial stage during the MIS 6b and 6c. An additional noteworthy observation within this interval is the presence of gastropod shells identified as Limacina retroversa (Jeanne Rampal, personal communication), recovered during sieving of a sample at 44 m, corresponding to around 155.5 ka BP (Fig. 4). This species is usually most abundant in temperate to subpolar waters in the North-Atlantic (Thabet et al., 2015). Zone 3 is mainly characterized by the abundance of Ericaceae and indicates cold and humid conditions at the final stage of MIS 6 (6b and 6a). Zone 4, at the end of MIS 6a, is divided into 3 subzones which display fast vegetation changes during the transition from MIS 6 to MIS 5 (Termination II), and Heinrich Stadial 11. The fast expansion of steppe and semi-desert taxa (Artemisia, Amaranthaceae, Ephedra) occurs simultaneously with the first increase of deciduous temperate and Mediterranean forest indicative of the initialization of interglacial conditions (zone 4a). This episode of arid vegetation dominance is interrupted in zone 4b by the fast expansion of montane vegetation mainly represented by Cedrus. A new steppe and semidesert vegetation increase is observed in zone 4c, while the deciduous temperate forest and the Mediterranean vegetation continue to expand. Finally, zone 5 is characterized by the maximum abundance of mesophilous and thermophilous elements, mainly represented by deciduous Quercus and Quercus ilex, typical of the MIS 5 interglacial optimum.

315

316317

21/

318319

320

320

321

322 323

324

325

326





Pollen zone	Depth (mcd) Age (ka BP)	and	Description of the pollen assemblage (Fig. 3)	Climate reconstructions (Fig. 5)		
5	40.25-39.98 m 128.73-127.47 BP	ka	Peak abundance of deciduous Quercus (up to 32%), Quercus ilex (4-10%), Olea (2-11%), Pistacia (up to 4%), aquatic herbaceous (up to 5%) and Isoetes (up to 38%). High values of Cichorioideae (up to 30%). Low percentages of Pinus (<35%), Artemisia (<11%), Amaranthaceae (<18%) and Ephedra (<3%).	Rapid increase of temperature, precipitation and seasonal contrast close to the modern value		
4c	41.08-40.28 m		,	First decrease, and then increase in temperatures		
	131.13-128.81 BP	ka	Amaranthaceae (up to 26%). High values of Cedrus (5-28%), and increasing percentages of deciduous Quercus (10-23%), Cichorioideae (0-14%) and Quercus ilex (1-13%). Decrease of Ericaceae (13-0%). Increasing percentages of Isoetes (0-5%) and Pteridophytes spores (0-17%).	and precipitations, with low PCON.		
4b	41.21-41.09 m		Peak abundance of <i>Cedrus</i> (up to 37%). Decrease of	Abrupt rise in precipitation contrast, but still cold		
	131.51-131.16 BP	ka	Artemisia (30-7%), Amaranthaceae (6-13%) and Ephedra (6-4%). Notable abundance of deciduous Quercus (6- 15%) and Quercus ilex (1- 3%).	conditions.		
4a	41.82-41.22 m		Peak abundance of Artemisia, (24-47%),	•		
	133.28-131.54 BP	ka	Amaranthaceae (14-6%) and <i>Ephedra</i> (5-11%). Decreasing trend of Ericaceae percentages (12-2%), and progressive increasing of deciduous <i>Quercus</i> (4-11%) and <i>Quercus ilex</i> (1-8%). Decrease of Cichorioideae	and seasonal contrast.		





			(<11%) and Cupressoideae (<8%).	
3	44.57-41.85 m 143.49-133.37 BP	ka	•	present), and important precipitations rise until values higher-than-present. Seasonal
2	48.91-44.63 m 165.16-143.68 BP	ka	High percentages of Cichorioideae (11-34 %), Poaceae (4-18%), Artemisia (4-37%), Amaranthaceae (3-16%) and Ephedra (3-12%). Cupressoideae maximum between 150-160 ka BP (up to 17%), and abundant Cedrus (up to 25%). Very low values of deciduous Quercus (<10%), Mediterranean taxa (<4%) and Ericaceae (<12%), with minimum values between 150 and 158 ka BP.	Decline of temperatures and precipitations, both lower than the modern values, reaching a minimum between ~164-155 ka BP. Afterwards, progressive rise in temperature, precipitation and seasonal contrast.
1	53.76-49 m 195.72-166.29 BP	ka	High percentages of Cedrus (8 to 45%) and deciduous Quercus (4 to 34%), with important variations. Abundant Cichorioideae (up to 43%) and Ericaceae (up to 25%), with notable presence of Abies (up to 5%), Quercus ilex (up to 6%) and Isoetes (up to 6%). Relatively low values of semi-desert elements (Artemisia, Amaranthaceae, Ephedra) but with two increases at 49.6 m /172 ka BP and at 51.6 m / 185 ka BP.	expressed by the smoothed lines, but important and numerous rapid oscillations. In general, values of precipitation and seasonal contrast are close or higher that the modern value, while temperature

Table 2: Description of the pollen zones identified through CONISS cluster analysis, including the main characteristics of their pollen assemblage and associated climate reconstructions.







Fig. 4: *Limacina retroversa* specimen found in sample B6H4 130-132 (identification: Jeanne Rampal personal communication). Photo: Dael Sassoon.

#### 4.2. Pollen-inferred climate reconstructions

Results show significant temperatures and precipitation variations in connection with the glacial / interglacial cyclicity and shorter-term variability (Fig. 5, Table 2). The most reliable methods according to the two R<sup>2</sup> and RMSE indicators are MAT and BRT, and the most accurately reconstructed parameters are MAAT and MTCO (Table 3). The four methods are in agreement for the general trends, although MAT shows the widest amplitude of variations, and RF has the smoothest curve.

Temperatures are lower than the present all along MIS 6, except at the onset of MIS 5. A cooling trend is reconstructed during the final stage of MIS 7 (pollen zone 1, MIS 6e and 6d), while MTCO and the seasonal temperature contrast (TCON) are stable. The methods do not agree on the precipitation patterns during this phase, with MAT showing a trend toward aridity, decreasing WINTERPR and seasonal precipitation contrast (PCON), while the three other methods display a slight precipitation increase and stable PCON. From 166 ka BP onward (pollen zone 2, MIS 6c and 6b), both temperatures and precipitation decrease, and the seasonal contrast between winter and summer climate conditions reduced progressively. The MIS 6 minimum temperatures and precipitation are reconstructed in pollen zone 2 between around 150 and 160 ka BP, corresponding to the transition between MIS 6c and 6b. Subsequently, both temperatures and precipitation increase progressively in the late pollen zone 2 and early pollen zone 3 (MIS 6b to 6a). Between 140-135 ka BP (early MIS 6a), the four methods reconstruct temperatures similar to late MIS 7, a seasonal contrast close to the present, and precipitation higher than the present (except for BRT). This climate optimum is abruptly interrupted by the HS11 extreme arid event between ~134 and ~129 ka BP (pollen



357

358 359

360



zone 4, late MIS 6a), during which temperatures, precipitation and seasonal contrasts are significantly reduced, reaching climate conditions similar to the MIS 6 glacial maxima ~155 ka BP. A short climate amelioration is evidenced at ~132 ka BP (pollen zone 4b), where precipitation and seasonal contrasts increase abruptly. Finally, after 130 ka BP the climate amelioration toward the MIS 5 interglacial conditions happens very fast (pollen zone 5).

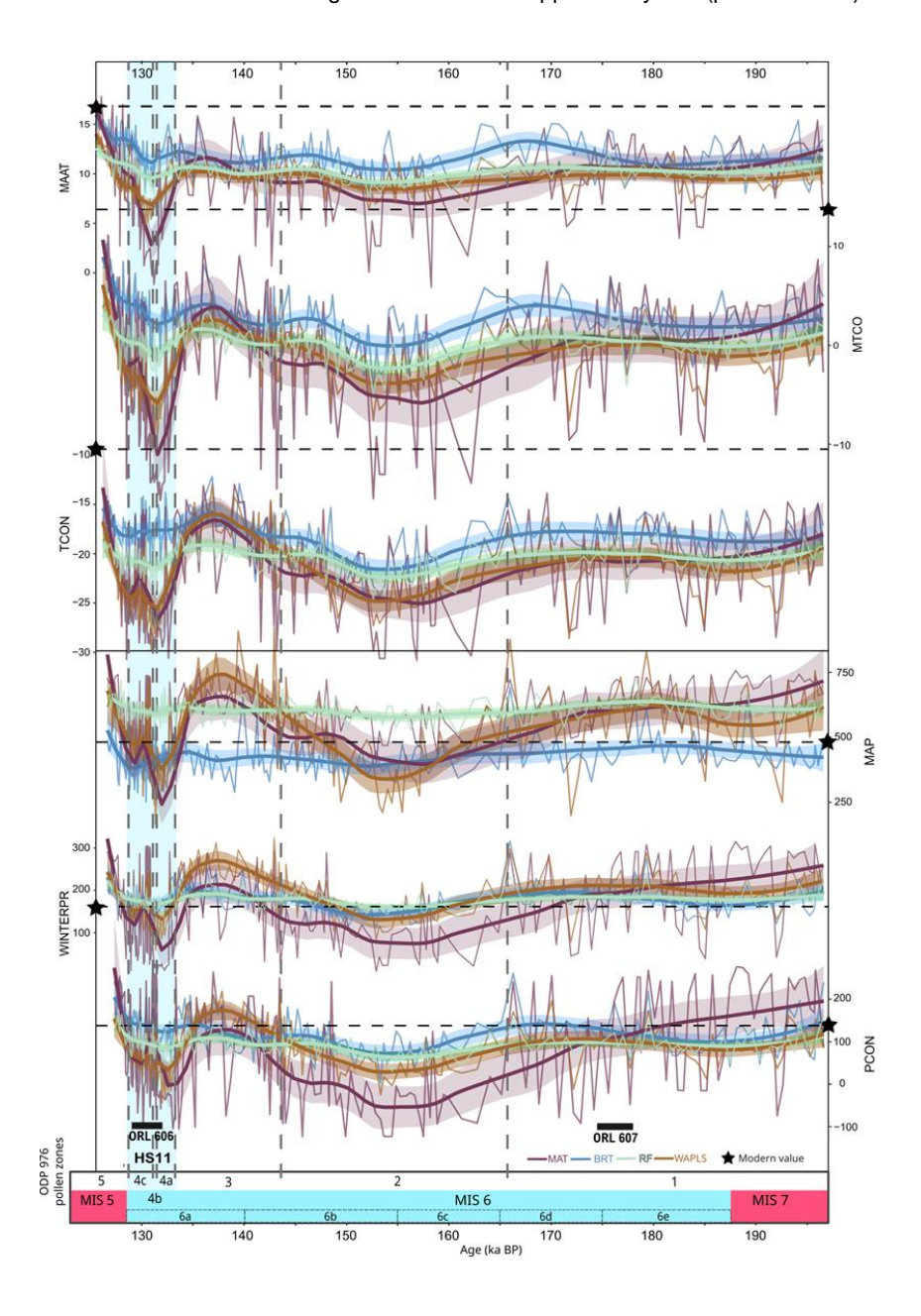






Fig. 5. Pollen-based climate reconstructions for MIS 6 interval in the ODP 976 record. MAAT (Mean Annual Temperature), MTCO (Mean Temperature of the Coldest Month), TCON (Temperature Contrast, see methods), MAP (Mean Annual Precipitations), WINTERPR (Winter Precipitations) and PCON (Precipitation contrast, see methods) for the four different methods applied: MAT (Modern Analogue Technique), WA-PLS (Weighted Averaging Partial Least Square), BRT (Boosted Regression Trees) and RF (Random Forest). The light-coloured interval represents the 95% confidence window, and the bold curves the loess smoothed values (alpha = 0.25). Modern values are indicated by the horizontal dashed line and the red star. Grey vertical dashed lines separate the pollen zones defined by CONISS cluster analysis.

	BRT		MAT		WA-PLS		RF	
	$R^2$	RMSE	$R^2$	RMSE	$R^2$	RMSE	$R^2$	RMSE
MTCO	0.87	2.96	0.88	3.19	0.71	4.44	0.77	3.88
MAAT	0.83	2.31	0.83	2.48	0.66	3.22	0.69	3.00
SUMMERPR	0.77	44.86	0.82	46.61	0.52	66.87	0.65	56.48
MAP	0.77	148.52	0.79	163.70	0.50	225.68	0.66	182.32
MTWA	0.76	2.25	0.79	2.33	0.53	3.16	0.61	2.81
WINTERPR	0.69	60.69	0.72	65.81	0.43	82.58	0.59	69.34

Table 3: R<sup>2</sup> (coefficient of determination) and RMSE (Root Mean Square Error) values for the different climate parameters reconstructed with the four methods applied. The lower the RMSE and the higher the R2, the more reliable the reconstruction.

## 5. Discussion

## 5.1. Paleoenvironment of MIS 6 and Termination II in the western Mediterranean

Important changes are recorded during MIS 6, that are consistent with orbital-scale variability during the different glacial substages and with D-O like dynamics.

Three phases can be discerned. The early phase (pollen zone 1) spans late MIS 7, MIS 6e and 6d and is characterized by high percentages of deciduous *Quercus*, *Cedrus* and Cichorioideae, with marked variability and abrupt semi-desert and steppe increases under cool and humid climate conditions, with seasonal contrast similar to present-day. The middle phase (pollen zone 2) extends from MIS 6c to late 6b, and displays the maximum expansion of steppe and semi-desert taxa together with very low temperatures and precipitation between ~160 and ~150 ka BP, a chronology compatible with the maximum Drenthe ice advance (Ehlers et al., 2011). Finally, the late phase (pollen zone 3), spanning late MIS 6b and 6a, is marked by a major expansion of Ericaceae vegetation associated with higher reconstructed precipitation and winter temperatures, as well as enhanced seasonal contrast during this phase.



393

394

395

396 397

398

399400

401

402 403

404 405

406 407

408

409

410

411 412

413

414

415

416

419

420 421

422

423 424

425

426 427



The final phase of MIS 6 is characterized by important changes in vegetation and climate, indicating a rapid reorganization of vegetation communities and atmospheric configuration at the transition between MIS 6 and MIS 5. Termination II (TII), defined as the period of fast reorganization of the climate system from full glacial (MIS 6) to full interglacial (MIS 5) conditions, is indeed characterized by extreme and fast internal dynamics including a major Heinrich Stadial, HS11 (Broecker & Henderson, 1998; Gouzy et al., 2004; Martrat et al., 2014, 2014; Moseley et al., 2015; Ovsepyan & Murdmaa, 2017). The Timing for TII has been estimated based on the initialisation and termination of Weak Asian Monsoon evidenced in the Dongge cave speleothems, lasting from ~136 to 129 ka BP (Bajo et al., 2020; Kelly et al., 2006; Menviel et al., 2019). These boundaries for TII give a total duration of about 7 ka. Approximately the same duration is observed in the Alboran Sea vegetation response to TII, but with ~1 ka delay. The imprint of HS11 on the vegetation in the Western Mediterranean region is recorded here between 133.3 - 128.8 ka BP (pollen zone 4). ODP 976 provides for the first time a very detailed record of vegetation successions during this arid event (pollen zones 4a, 4b and 4c), in agreement with other SSTs and speleothem records that depict a three-phases or "double U" pattern for the event (see section 5.4). After the first rapid increase of steppe and semi-desert taxa (pollen zone 4a), the middle phase shows an abrupt decrease of steppe and semi-desert vegetation, and a fast increase of montane trees (mainly Cedrus) percentages (pollen zone 4b). Climate reconstructions reflect this event through a fast increase of both precipitation and temperatures. This pattern is fully compatible with the ODP 976 SSTs trend (Jiménez-Amat and Zahn, 2015; Martrat et al., 2014), although a delay of about 1 kyr is observed between the abrupt drop in alkenone-based SST and the expansion of steppe and semi-desert vegetation. The same way, the abrupt sea surface warming in the middle of HS11 (~133 ka BP) is shifted in the pollen record, to around 131.5 ka BP (pollen zone 4b).

#### 5.2. Atmospheric connection with ORLs deposition during MIS 6

417 418

Pollen analyses help us to characterize the processes behind Organic Rich Layers (ORLs) deposition in this western Mediterranean region. Like sapropels, they reveal important changes in the water stratification and circulation, with reduced bottom water ventilation and enhanced organic productivity in straight connection with (i) increase in the freshwaters Atlantic inflow at times of deglaciation and (ii) enhanced rivers runoff regionally linked with increased precipitation (Murat, 1999; Pérez-Asensio et al., 2020; Rogerson et al., 2008). Although they are often considered as "ghost sapropels", their timing and the mechanism behind them may differ from those of Eastern Mediterranean sapropels (Rogerson et al., 2008). ORL bed 607 coincides with a period of enhanced precipitation around 176 ka reconstructed through our pollen-based approach (Fig. 7). Its basis appears almost synchronous with the onset of

https://doi.org/10.5194/egusphere-2025-5024 Preprint. Discussion started: 21 October 2025 © Author(s) 2025. CC BY 4.0 License.





Sapropel S6 layer deposition in the Eastern Mediterranean (Emeis et al., 2003; Rohling et al., 2015; Savannah et al., 2024). Its duration also appears shorter than Sapropel S6, possibly indicating an interruption of favourable climate conditions in the Western Mediterranean region by a stadial event occurring around 172 ka BP and marked by an abrupt decrease in precipitation (Fig. 7). ORL bed 606 was deposited during the second half of Termination II, at a time of deglaciation and directly following the first aridity pulse of HS11. Pollen-based reconstructions show enhanced precipitation and seasonal contrast during this time, suggesting intense precipitation together with deglacial freshwater input as combined causes for ORL deposition in the Western Mediterranean, which finds no counterpart in the Eastern Mediterranean. The implications of such organic layer deposition occurring at times of enhanced precipitations or deglaciation will be furtherly discussed in section 5.4.

5.3. Mediterranean vegetation changes during the penultimate glaciation: a synthesis

The ODP 976 pollen record documents MIS 6 vegetation changes in the Western Mediterranean with a temporal resolution comparable to the most detailed terrestrial palynological sequences from the Eastern Mediterranean (Tenaghi Philippon and Ioannina). This W-E transect of Mediterranean palynological records offers valuable insights on the spatial pattern of vegetation changes during the penultimate glaciation (Fig. 6).





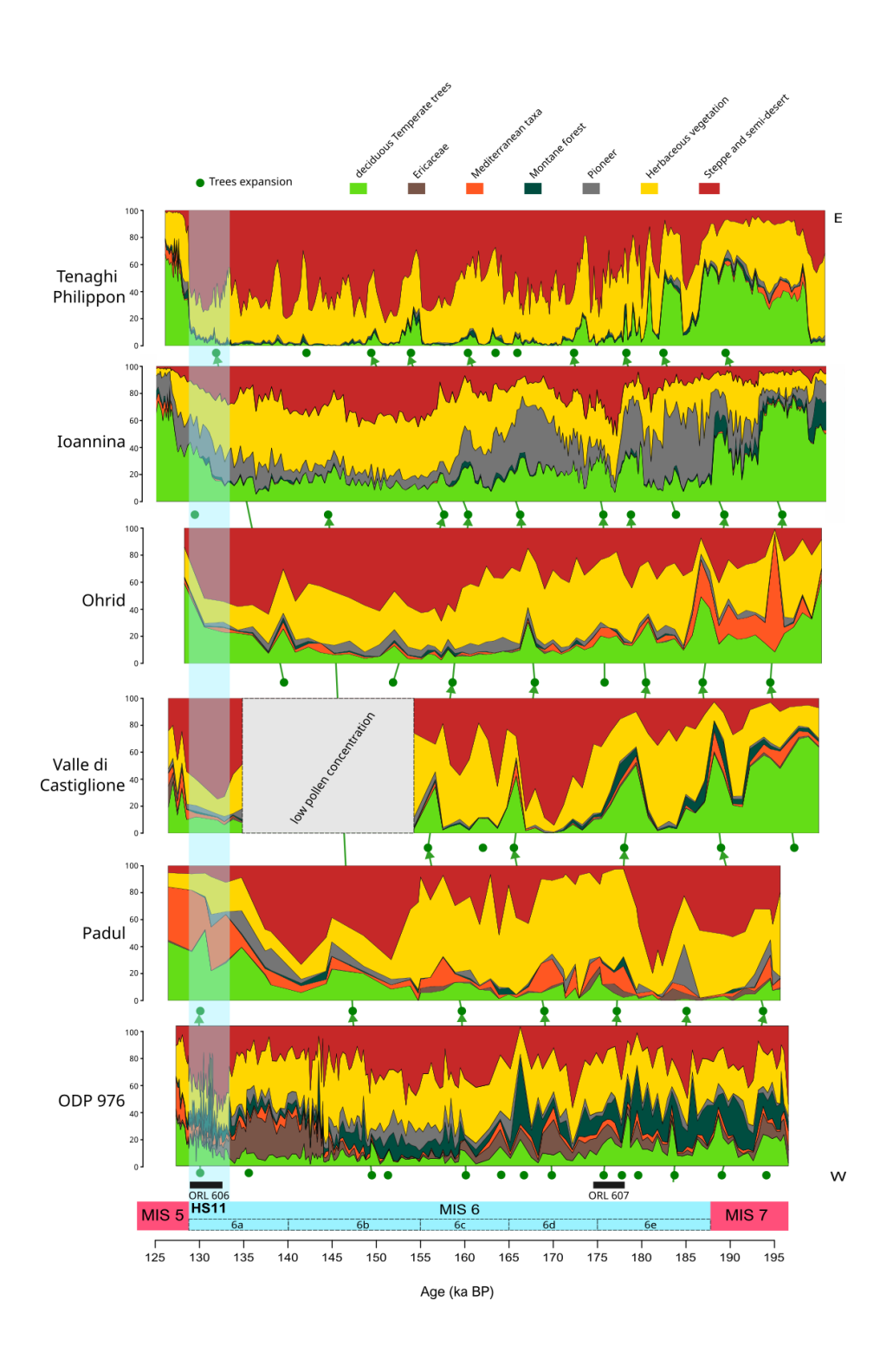






Fig. 6. Synthesis of vegetation changes in the Mediterranean during MIS 6 based on available palynological sequences, from east (top) to west (bottom): ODP 976 (this study), Padul (Camuera et al., 2019), Valle di Castiglione (Follieri et al., 1988), Ohrid (Sadori et al., 2016), Ioannina (Roucoux et al., 2011), Tenaghi Philippon (Koutsodendris et al., 2023). Each synthetic pollen diagram is plotted according to its own age model. ODP 976 and Ioannina's chronologies are based on alignment with MD01-2444 temperate pollen curve on AICC2012 timescale. The ecological groups are the same as for ODP 976, except *Pinus* was included in pioneer vegetation at Ioannina. Green dots indicate temperate vegetation increases, with tentative correlations between records. The two Organic Rich Layers (ORLs) identified in the ODP 976 core (Murat, 1999), were placed at the bottom.

At the MIS 7-6 transition, no abrupt decline of temperate forest is recorded in the ODP 976 and Padul records, in contrast with central and Eastern pollen records such as Tenaghi Philippon, Ioannina, Ohrid and Castiglione where the transition is very abrupt (Follieri et al., 1988; Koutsodendris et al., 2023; Roucoux et al., 2011; Sadori et al., 2016). This difference is probably linked with the lower percentages of deciduous forest in the Western Mediterranean region.

The first half of MIS 6 (~185-165 ka BP) is marked by relatively high percentages of arboreal pollen across all records, especially deciduous forest (Roucoux et al., 201; Margari et al., 2010, 2014). The abundance of montane taxa (mainly *Cedrus*) is characteristic of ODP 976 record, and reflects the development of altitudinal trees on the Moroccan Rif mountains. Montane elements also increase during early MIS 6 at Valle di Castiglione, mainly represented by *Fagus* and *Abies* (Follieri et al., 1988), and at Ioannina, mainly represented by *Pinus* (Roucoux et al., 2011). No equivalent pattern is recorded in Padul where herbaceous vegetation is largely dominant. The scarcity of palynological data from the western Mediterranean, especially from North Africa, limits our understanding of the spatio-temporal significance of *Cedrus* expansions during MIS 6, and past glaciations in general.

The main phase of steppe and semi-arid vegetation is recorded between ~165-145 ka BP in the Alboran Sea record, consistent with Ohrid and Ioannina pollen sequences (Fig. 6). In Padul, however, the maximum expansion of steppe and semi-desert taxa occurs later, between ~155 and ~137 ka BP. This time window corresponds to the glacial maximum recorded at Azzano X (northern Italy) between 148 and 135 ka BP (Pini et al., 2009), and to a period of low pollen concentration at Valle di Castiglione, likely reflecting full glacial conditions. The ~10 ka lag in the vegetation glacial maxima between ODP 976 and Padul is probably the result of the low temporal resolution of the latter, in addition to differences in the age models used. However, the presence of pioneer vegetation and to a lesser extent of montane elements in Padul during the maximum glacial phase matches the ODP 976 pattern in pollen zone 2, where Cupressoideae and *Cedrus* display high abundance.



478

479

480

481

482

483

484 485

486

487

488 489

490 491

492

493

494

495

496

497

498

499

500

501 502

503

504

505

506

507

508 509

510

511

512



A distinctive feature of the Western Mediterranean vegetation recorded during the final stage of MIS 6 (pollen zone 3) is the marked increase in Ericaceae observed in ODP 976 record, and almost absent in the rest of the Mediterranean region. A similar expansion is observed in the Atlantic margin, where core MD01-2444 recorded patterns of Ericaceae expansion matching the three insolation minima during MIS 6 (Margari et al., 2014). The expansion of heathland vegetation in the Iberian Peninsula as recorded in ODP 976 during the final stage of MIS 6 therefore marks the renewed influence of westerlies and Atlantic moisture preceding the onset of the transition to MIS 5 interglacial (Margari et al., 2014). Supporting this interpretation, an increase in temperate deciduous forest at the end of MIS 6 is also seen in Padul, Ohrid and Joannina records before the transition to MIS 5.

Despite some discrepancies due to the differences in age models and temporal resolutions, all records display comparable variations in temperate pollen percentages during the penultimate glacial. These variations support the persistent sensitivity of Mediterranean plant ecosystems to global-scale millennial climate variability during the penultimate glaciation, with modulation of the vegetation response depending on the local geography. Strong similarities can be observed between ODP 976 and Padul, despite the lower temporal resolution of Padul record. In both sequences, temperate pollen percentages reached ~25 % of total pollen as a maximum during the rapid forest expansions events in the first half of MIS 6. This similarity supports the validity of the ODP 976 marine record to reconstruct the SW Iberian Peninsula temperate forest history. However, ODP 976 sequence provides a more regional image of the vegetation, including higher percentages of Ericaceae pollen coming from the Atlantic coast, and Cedrus pollen from the Moroccan Rif mountains (Jiménez-Moreno et al., 2020), compared to Padul where percentages of Mediterranean taxa and hygrophyte herbaceous are higher due to the local nature of the signal (Camuera et al., 2019). Looking further east, Valle di Castiglione recorded various temperate trees expansions and contractions during the lower MIS 6, before the full glacial conditions. In the Italian Peninsula, various interstadials have also been identified further north at Azzano X (Pini et al., 2009). In the Balkans, Tenaghi Philippon shows the highest percentages of semi-desert and herbaceous vegetation across MIS 6, with more abrupt changes than all the other Mediterranean records, and more amplitude of the trees' contractions. This reflects the exacerbated vegetation dynamics locally, with episodes of rapid colonization by tree vegetation and probably linked with the lower altitude of the site (Koutsodendris et al., 2023). On the contrary, the Ioannina record shows the highest deciduous forest percentages of all the records presented here, supporting its character as a local trees refugium (Roucoux et al., 2011).

Termination II displays a particular pattern in vegetation records from the Mediterranean region: while the expansion of trees and temperate vegetation is fast and





continuous, HS11 represents at the same time a remarkable episode of abrupt steppe and semi-desert expansion. Although this event is visible in almost all the records, it is particularly prominent in ODP 976 record (pollen zone 4), and appears less pronounced in the eastern Mediterranean sequences. In Padul, no major expansion of xerophyte vegetation is detected, but a small decrease of temperate deciduous taxa was interpreted as the HS11 imprint (Camuera et al., 2019), and the signal might be hindered by the low resolution of the record. A pattern of fast arid vegetation increase contemporaneous to the temperate forest expansion is also found in central Italy at Lago Grande di Monticchio, which was not presented in Fig. 6 as its record does not extend beyond 132 ka BP (Allen and Huntley, 2009; Brauer et al., 2007).

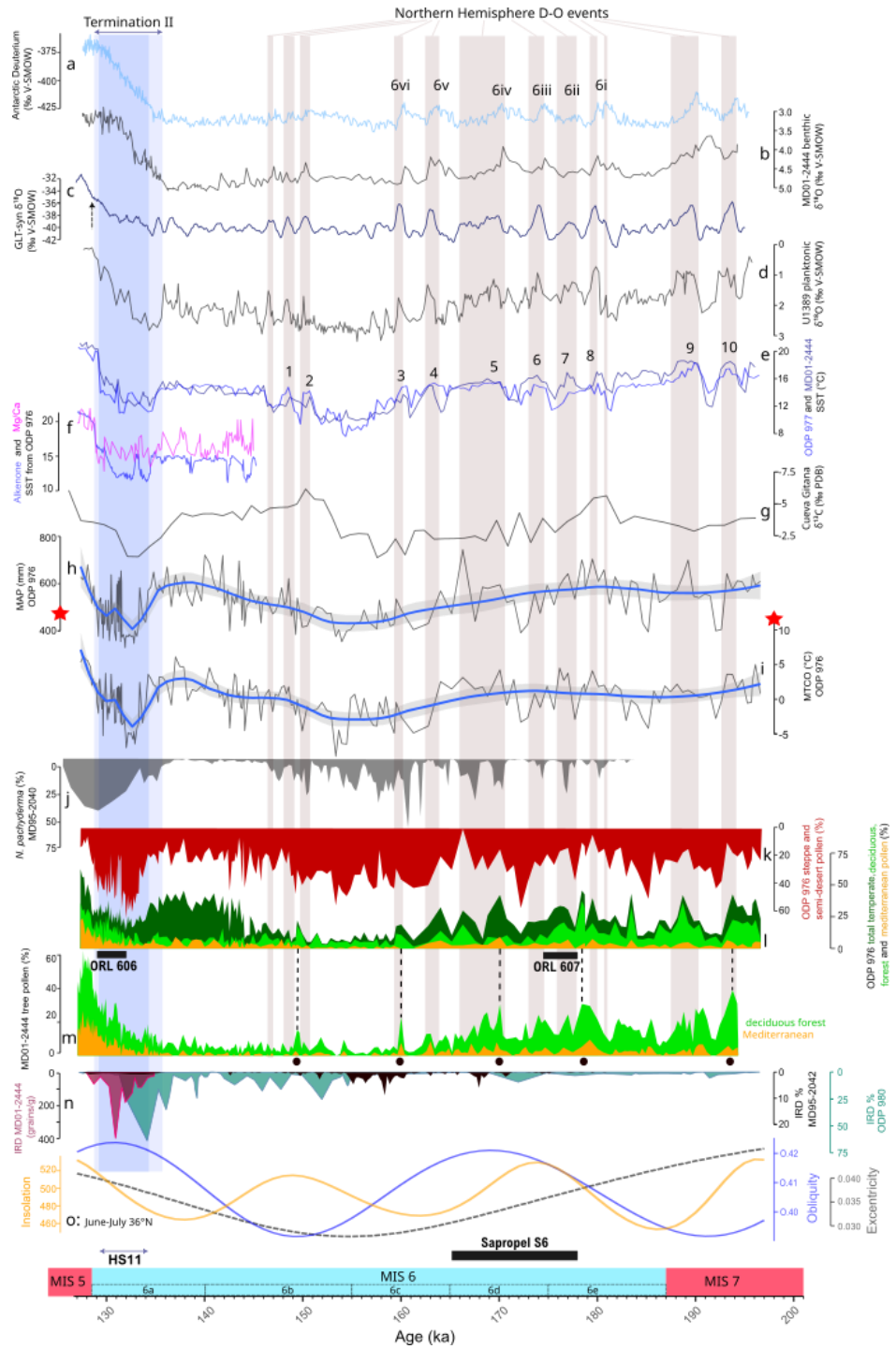
To sum up, all palynological sequences reveal high-frequency oscillations of temperate and semi-desert pollen, compatible with DO-like variability, and which are a particularly distinctive feature of the lower part of MIS 6.

## 5.4. Rapid climate variability during MIS 6: a regional multiproxy comparison

In order to disentangle the character of rapid climate variability during MIS 6, a comparison with regional and global climatic archives is essential. The increases in arboreal pollen observed in the ODP 976 record are consistent with those from the Portuguese margin core MD01-2444 (Margari et al., 2010, 2014; Tzedakis et al., 2018) (Fig. 7). However, the ODP 976 record generally presents lower percentages of temperate deciduous pollen percentages compared to the Atlantic record, due to the Mediterranean influence as previously evidenced for the last glacial period (Charton et al., 2025; Fletcher et al., 2010). To better capture temperate vegetation dynamics, we added Ericaceae, a clear marker of Atlantic influence in the ODP 976 record, to the deciduous temperate forest, to obtain a "total temperate pollen sum" which enhances the main warming peaks and strengthens the correlation between the two marine cores on both sides of Gibraltar Strait (Fig. 7). Another striking correlation appears between the ODP 976 pollen-inferred climate reconstructions, the SSTs trends based on alkenones (Martrat et al., 2004, 2007), and the speleothem data from Cueva Gitana (Hodge et al., 2008) (Fig. 7). The ODP 976 pollen record therefore appears to reflect well regional variations in both temperature and humidity across MIS 6.







Age (ka) Fig. 7: Millennial climate changes during MIS 6. a) Antarctic Dome C δD (Bazin et al., 2013; Jouzel et al., 2007); b) Benthic  $\delta^{18}$ O from MD01-2444 (Margari et al., 2010); c) Greenland

https://doi.org/10.5194/egusphere-2025-5024 Preprint. Discussion started: 21 October 2025 © Author(s) 2025. CC BY 4.0 License.





synthetic  $\delta^{18}$ O (Barker et al., 2011); **d)** Planktonic  $\delta^{18}$ O from U1389 (Sierro and Andersen, 2022); e) alkenone-based SST from ODP 977 (darker blue) and MD01-2444 (lighter blue) (Martrat et al., 2004, 2007); f) Alkenone-based SST (Martrat et al., 2014) and Mg/Ca-based SST (Jiménez-Amat and Zahn, 2015) from ODP 976; g)  $\delta^{18}$ C from Cueva Gitana (Hodge et al., 2008); h) Mean Annual Precipitation (MAP) reconstructed from ODP 976 pollen assemblage, mean of the four methods used in this study (MAT, WA-PLS, RF, BRT), with the red star showing the modern value; i) Mean Temperature of the Coldest Month (MTCO) reconstructed from ODP 976 pollen assemblage, mean of the four methods used in this study (MAT, WA-PLS, RF, BRT) ), with the red star showing the modern value; i) N. pachyderma percentages from MD95-2040 (de Abreu et al., 2003); k) ODP 976 pollen percentages of semi-desert and steppe taxa (this study); I) ODP 976 pollen percentages of total temperate taxa including temperate deciduous forest + Ericaceae + Mediterranean (dark green), deciduous forest (light green), Mediterranean (orange) (this study); m) MD01-2444 pollen percentages of temperate tree (light green) and Mediterranean (orange) taxa (Margari et al., 2010; Tzedakis et al., 2018); n) Ice-Rafted Debris (IRD) percentages from MD01-2444, 37° N (pink) (Skinner & Shackleton, 2006) redrawn from Tzedakis et al. (2018), MD95-2040 (red), 40°N (de Abreu et al., 2003) and ODP 980 (blue), 55°N (McManus et al., 1999; Oppo et al., 2001, 2006); o) orbital parameters (Laskar et al., 2004) calculated for June-July at 36°N: Eccentricity (black), Obliquity (blue) and Insolation (yellow). The black rectangle indicates the interval of deposition of Sapropel layer S6 in the eastern Mediterranean (Ziegler et al., 2010). The marine substages MIS 6a-e follow (Railsback et al., 2015). All data are plotted on AICC2012 chronology (Bazin et al., 2013) following Sierro et al. (2020, 2022), except for the IRD records and Gitana Cave, which is plotted on its own age model based on U-series absolute dating. The vertical grey bars indicate the Northern Atlantic interstadial events based on the planktonic isotope record and the predicted D-O events from Greenland synthetic record, with the numbers of the Alboran interstadials (Al-1 to Al-10) from Martrat et al. (2004, 2007). Numbers 6i-6vi correspond to the Antarctic Isotope Maxima (AIM) from Margari et al. (2010). The vertical blue bar represents Heinrich Stadial 11 (HS11), Black dots and dotted lines show the five temperate pollen peaks in MD01-2444 used as control points for ODP 976 chronology.

542

543

544

545

546 547

548

549

550

551

552

553

Warm events in the northern hemisphere are generally well-correlated to peaks in the ODP 976 temperate pollen curve. An active bipolar seesaw dynamics was described during the penultimate glacial (Davtian & Bard, 2023; EPICA Community Members, 2006; Stocker, 1998), and the Antarctic record was used to elaborate the Greenland  $GL_T$ -syn (Greenland temperature synthetic) curve showing predicted  $\delta^{18}O$  D-O events for the past glacial eight climatic cycles, which are not directly recorded in Greenland ice (Barker et al., 2011; Bazin et al., 2013; Jouzel et al., 2007). Six Antarctic Isotopic maxima (AIM) events were recognized on the Deuterium curve during MIS 6 (6i to 6vi), correlated with increases in CO2 concentrations and benthic isotope minima in the North Atlantic (Barker et al., 2011; Hodell et al., 2023; Margari et al., 2010, 2014; Shin et al., 2020) (Fig. 7). These AIM and benthic minima in the Atlantic are not easily correlated with steppe expansions in the ODP 976 record, indicating a limited response of vegetation in the Western Mediterranean to the Antarctic warm events.



557

558

559

560

561

562

563 564

565

566

567

568

569 570

571

572

573

574575

576

577

578

579

580 581

582 583

584 585

586

587

588

589

590 591



Barker et al. (2011) predicted the occurrence of eleven D-O events during MIS 6, while nine interstadials were recognized in the Alboran Sea from the alkenone record (Martrat et al., 2004, 2007). In the loess record of Harletz in central Europe, ten interstadials were described (Rousseau et al., 2020), strongly matching the Chinese speleothems records of stadial and interstadial events related to the Asian Monsoon dynamics (Cheng et al., 2006; Li et al., 2014; Wang et al., 2018; Wang et al., 2001; Xue et al., 2019). The global nature of fast climate oscillations in the northern hemisphere thus appears controlled by the coupled influence of Atlantic cold events, and tropical monsoon variations as evidenced by the eastern Mediterranean speleothems records from Sofular, Soreq and Kanaan caves (Ayalon et al., 2002; Held et al., 2024; Matthews et al., 2021; Nehme et al., 2018).

MIS 6 is traditionally divided into three phases characterized by different general trends and amplitude of millennial-scale oscillations (Margari et al., 2014; Nehme et al., 2020). Margari et al. (2014) described an early phase between 185 and 160 ka BP, with warmer and wetter conditions and important rapid climate variability, a middle transitional phase between 160 and 150 ka BP, and a late phase with stable glacial conditions between 150 and 135 ka BP. This three-phasing for MIS 6 glaciation matches our interpretation of ODP 976 pollen zones 1, 2 and 3.

Early MIS 6 (187-166 ka BP): warm/wet conditions and instability. The first phase encompasses the two substages MIS 6e and 6d, and is characterized by humid and rather warm climate conditions in the Mediterranean at the transition from MIS 7 to MIS 6. This phase aligns well with the deposition of ORL bed 607 in the Alboran Sea, and the sapropel layer S6 in the Eastern Mediterranean, associated with the maximum summer insolation and increased intensification of the summer monsoonal system in the eastern Mediterranean between 178.5 to 165.5 ka (Emeis et al., 2003; Rohling et al., 2015; Ziegler et al., 2010). At the same time of S6 deposition, Cheddadi and Rossignol-Strick (1995) described an increase in temperate pollen in the Nile region, and Soreq cave speleothem records climatic conditions typical of an interglacial (Ayalon et al., 2002). Sapropel depositions usually occur during interglacial periods as MIS 1 (Holocene), which makes sapropel S6 an exceptional feature of early MIS 6. It reflects particularly warm and humid conditions, and intense freshwater input in the Mediterranean which can result from various sources, including increased rainfall and monsoon activity, Atlantic freshwater entrance, and enhanced river discharges (Sierro and Andersen, 2022). The long speleothem records in China report a period of northern shift of the Intertropical Convergence Zone associated with enhanced Asian Monsoon activity during this phase (Wang et al., 2018). Higher pluviometry is supported by foraminifera isotopic and SSTs signal throughout the Mediterranean Sea (Kallel et al., 2000). Enhanced rainfall in the Balkans is evidenced by the Ioannina lake deepening (Wilson et al., 2021), and a more humid period is https://doi.org/10.5194/egusphere-2025-5024 Preprint. Discussion started: 21 October 2025 © Author(s) 2025. CC BY 4.0 License.



592

593

594

595

596 597

598 599

600

601 602

603

604

605

606

607

608

609

610

611

612613

614

615

616 617

618

619

620

621

622

623 624

625

626



documented in speleothem records from Argentarola cave in Italy (Bard et al., 2002) and Gitana cave in southern Spain (Hodge et al., 2008) (Fig. 7). Therefore, humid conditions during this phase were not restricted to the eastern Mediterranean where the sapropel deposition occurred. ODP 976 organic layer 607 together with the pollen-based climate reconstructions support this view, with enhanced seasonal precipitation contrast during this interval driven by enhanced winter precipitations (Fig. 5). Comparison with Padul pollen-based hydroclimate reconstructions (Camuera et al., 2022) further strengthens this scenario: despite the chronological delay between the two sequences, this early MIS 6 humid phase and ORL deposition likely matches the Western Mediterranean Humid Period (WMHP 6) dated between 180-155 ka BP (Fig. 8). The same study made the case for a co-occurrence of humid periods in the Western Mediterranean and in West Africa (African Humid Periods) during periods of high precipitations seasonality and enhanced West African Monsoon. Pollen-inferred climate reconstructions from lake Ohrid have also shown the phase relationship between African Monsoons and periods of high winter precipitations in the Mediterranean region (Wagner et al., 2019; Sinopoli et al., 2019).

Another characteristic of this early MIS 6 phase is the strong variations in pollen and isotopic curves in the Atlantic and Western Mediterranean (Fig. 7). Variations in temperate deciduous and Ericaceae percentages are observed in the ODP 976 record, in close correspondence with the Atlantic record from MD01-2444. The largest interstadial peak in ODP 976 around 179 ka BP is also identified in all the different records and marked by warmer conditions in the sea, and more effective precipitations in SE Iberia (Hodge et al., 2008). It is well correlated with the stadial following Antarctic event 6i (Margari et al., 2010), the associated predicted D-O event in Greenland synthetic curve, and the Alboran Sea SST interstadial event 8 (Martrat et al., 2004). In Padul record, the temperate deciduous, Mediterranean and Abies percentages increase correlates well with this event (Camuera et al., 2019). It could also match the WMHP 6.1 interstadial (Camuera et al., 2022) (Fig. 8). This large interstadial was suggested to be at the origin of the initialisation of the sapropel S6 deposition (Sierro and Andersen, 2022), and could also have participated in the initialization of ORL 607 deposition in the Alboran Sea (Murat, 1999). On the other hand, the most important tree population decline and semi-desert expansion in ODP 976 is recorded at ~172 ka BP, which could match Antarctic event 6iv, and is associated to a moderate increase of IRD deposition at the latitude of ODP 980 (Fig. 7). A similar stadial can be observed in the Ioannina and Tenaghi Philippon records with a close chronology (Roucoux et al., 2011) (Fig. 6). Dry conditions at this time are also recorded in the eastern Mediterranean as shown in the Pentadactylos and Soreq speleothems (Ayalon et al., 2002; Nehme et al., 2018).



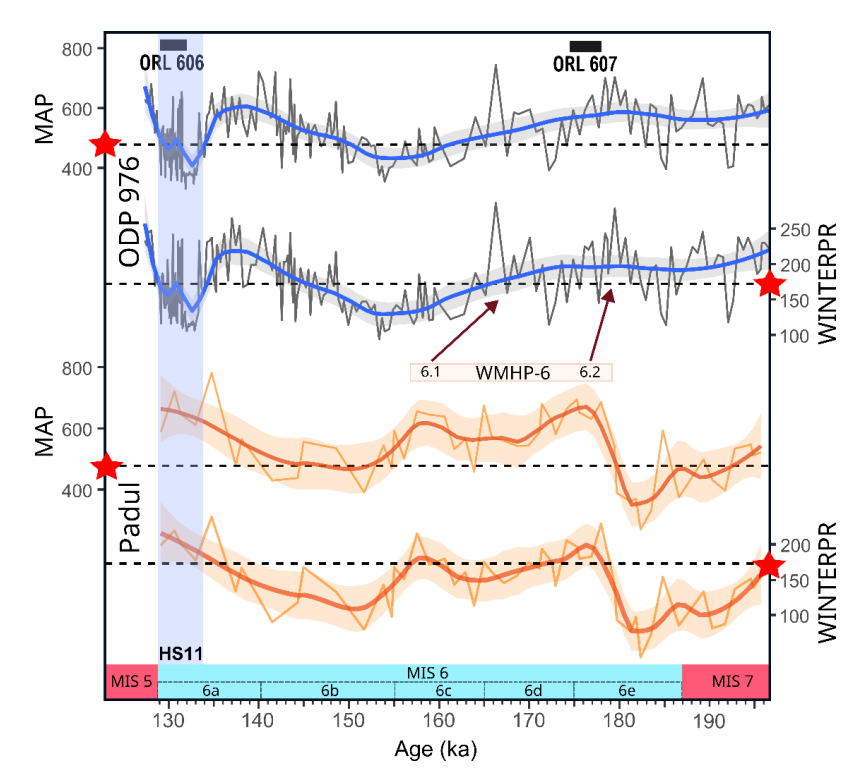


Fig. 8 Comparison between the precipitation pattern reconstructed from ODP 976 with our multi-method approach (mean) (this study) and from Padul with only the WA-PLS method (Camuera et al., 2022). Mean Annual Precipitation (MAP) and Winter Precipitation (WINTERPR) are represented, together with the two Organic Rich Layers (ORLs) identified in ODP 976 (Murat, 1999) and the Western Mediterranean Humid Period (WMHP) 6 defined by Camuera et al. (2022). Red arrows indicate tentative correlation between the two phases of WMHP 6, and the precipitation reconstructions from ODP 976. Red stars and dashed lines indicate the modern climate value (see methods).

Middle MIS 6 (165-144 ka BP): maximum glacial conditions and stability. This phase is marked by the maximum expansion of semi-desert vegetation and the almost complete collapse of forest vegetation between ~163 and 150 ka BP, according to the ODP 976 pollen and MD01-2444 records, synchronous with the minimum in orbital eccentricity. This is in agreement with the lowest SSTs values reconstructed in the Alboran Sea from the alkenone record occurring around 155 ka BP, and low SSTs in the Gulf of Lions too (Cortina et al., 2015). At the same time, high percentages of the cold species *N. pachyderma*, together with important ice-detritus pulses, are recorded on the Portuguese margin (de Abreu et al., 2003). The occurrence of the cold Atlantic species *Limacina retroversa* shells in the ODP 976 sediments





at ~155 ka BP is consistent with the enhanced entrance of cold subpolar water masses in the Alboran sea at the time of full glacial conditions. In parallel, there is an intensification of "Fleuve Manche" paleo river discharges evidenced in various sedimentary cores from the Bay of Biscay (Boswell et al., 2019; Eynaud et al., 2007; Penaud et al., 2009, 2016; Toucanne et al., 2009), and a fluvial aggradation linked with reduced vegetation cover in Spanish river basins (Macklin et al., 2002). A long-term aridification is recorded in SE Spain in Gitana cave close to the ODP 976 location (Hodge et al., 2008). The glacial maximum in Soreg cave speleothem is also recorded around 154 ka BP (Bard et al., 2002), and might be responsible for the hiatus in the Pentadactylos speleothem in Cyprus (Nehme et al., 2020). In Italy, the Tana che Urla cave also recorded cooling and aridification between 159-132 ka BP, indicated by both the carbon and oxygen isotopic ratio (Regattieri et al., 2014). The coolest phase in Abaliget Cave speleothem in central Europe is also recorded at that time (Koltai et al., 2017). Climate conditions reconstructed at ODP 976 site during this phase show the maximum aridity and cold temperatures, which are consistent and fall within the range of reconstructed temperatures and precipitations at the same time at Ohrid (Sinopoli et al., 2019). This main phase of glaciation in Europe took place after 163 ka BP, corresponding to the Drenthe glacial advance (Ehlers et al., 2018; Margari et al., 2014). The maximum ice expansion probably led to the almost complete collapse of temperate vegetation across the Mediterranean region, except in specific climate refugia's like Ioannina or Padul (Fig. 6). The Mediterranean vegetation taxa were particularly affected and almost disappeared at this time in the ODP 976 record.

Few interstadial events are observed during this cold and dry phase, probably due to the extended ice volume reaching a critical threshold (McManus et al., 1999) and leading to higher climate stability at time of glacial maximum expansion (Sierro and Andersen, 2022). One moderate interstadial event around 150 ka BP is expressed in the ODP 976 and MD01-2444 records through an increase in temperate deciduous tree taxa (Fig. 7). It may correspond to the interstadial recognized in Gitana Cave speleothem approximately at the same time, and is compatible with the Alboran Interstadial events 1 or 2 (Martrat et al., 2004), while a larger trees increase in Padul record is also observed (Camuera et al., 2019) (Fig. 6). It is also compatible with interstadials recognized in other speleothem records in eastern and central Mediterranean (Ayalon et al., 2002; Bard et al., 2002; Regattieri et al., 2014). Sierro et al. (2022) described a major event of low Mediterranean overturning and high freshwater entrance through the Gibraltar Strait at that time and contemporaneous to the insolation maximum (Fig. 7). This configuration was similar to the one contemporaneous to sapropel S6 and ORL 607 deposition during early MIS 6, but did not lead to any new sapropel deposition at 150 ka BP, probably because the climate conditions were more favourable but not enough for a sapropel deposition.



674

675

676

677

678

679

680 681

682 683

684

685

686

687

688

689

690

691

692

693

694

695

696

697 698

699

700

701 702

703

704 705

706

707

708



Late MIS 6 (144-129 ka BP): increased precipitation during the last glacial, and arid conditions during Heinrich Stadial 11. Between 150 and 140 ka BP, warmer and wetter conditions are indicated by ODP 976 pollen percentages of Ericaceae (pollen zone 3). Ericaceae expansions in the Iberian margin sediments were found to be associated to insolation minima in core MD01-2444 (Margari et al., 2014). This pattern is consistent with the ODP 976 Ericaceae curve (Fig. 7). The climate reconstructions evidenced high precipitations and especially high WINTERPR values. These higher humidity and temperature values are supported by the carbon isotope record from Gitana Cave (Hodge et al., 2008) and the Alboran Sea SSTs (Martrat et al., 2007). In central Europe, Abaliget Cave speleothem also show more favourable climate conditions during this phase (Koltai et al., 2017). Climatic oscillations appear subdued in the Western Mediterranean pollen records during this last phase. The high resolution ODP 976 record shows some SST variations (Jiménez-Amat and Zahn, 2015; Martrat et al., 2014): Ericaceae pollen contractions and semi-desert elements expansions could be correlated to three abrupt drops in alkenone-based SSTs at 144, 142, and 139 ka BP (Fig. 7). Fifteen Chinese Interstadials (CIS) were identified at Hulu Cave during late MIS 6, linked with Asian Monsoon dynamics (Q. Wang et al., 2018), and the ultra-high-resolution record of planktonic isotope ratio at U1389 by Sierro and Andersen (2022) also expresses some variability. However, the vegetation response in the SW Mediterranean was apparently limited.

Following the Ericaceae expansion, the most prominent feature of the late MIS 6 phase is the large and fast expansion of steppe and semi-desert vegetation during HS11, between 133 and 129 ka BP (pollen zone 4). It is characterized by a first large IRD peak at high latitude (ODP 980) around 134 ka BP, and later at the MD01-2444 latitude, around 131 ka BP (Skinner & Shackleton, 2006; Tzedakis et al., 2018). This event also corresponds to an increase in the oxygen isotopic ratio at the Portuguese margin (especially planktonic, starting around 136 ka BP), also broadly synchronous to an important decrease in SSTs of the Atlantic and the Mediterranean Sea (Jiménez-Amat and Zahn, 2015; Martrat et al., 2004, 2007, 2014). Climate reconstructions show particularly harsh conditions in the Western Mediterranean region during this event, compatible with the reconstructions from Lake Ohrid (Sinopoli et al., 2019) and from three French sites (Les Echets, la Grande Pile and Le Bouchet) for the latest phase of MIS 6 (Guiot et al., 1989, 1993). An arid phase is also evidenced at Gitana Cave (Hodge et al., 2008), which closely matches the trend of the ODP 976 precipitation curve (Fig. 8). Aridity is evidenced in other speleothem records in Europe like Villars (Wainer et al., 2011), Sieben in the Alps (Moseley et al., 2015), and Abaliget cave in central Europe (Koltai et al., 2017). Dryness over western Europe is also supported by an episode of intense loess deposition in Rodderberg crater in northern Germany between 136-129 ka BP (Zhang et al., 2024). If HS11





is also recorded in China speleothems (Wang et al., 2018), it appears subdued in the eastern palynological Mediterranean records (Fig. 6), indicating that the Western Mediterranean region was more severely impacted by the dry and cold pulse of HS11. The "double u" shape of HS11 described in section 5.1 for the ODP 976 record matches well the Hulu cave record, where the particular event in the middle of HS11 was linked with a strong Asian Monsoon episode that could represent an analogue to the Bølling-Allerød during Termination I (Wang et al., 2018).

HS11 has been described as a "pause" in the glacial termination II (Gouzy et al., 2004; Hodge et al., 2008). However, in the ODP 976 and MD01-2444 records, temperate vegetation keeps increasing all along the event, despite the supposed cessation of the warming and moistening trend for almost 2000 years. Therefore, the trend toward increased temperate vegetation during Termination II did not seem to be strongly affected by the abrupt arid event, following the continuous climate amelioration described in various speleothem records from Italy covering Termination II, at Corchia cave, Tana che Urla and Argentarola (Bard et al., 2002; Drysdale et al., 2005; Regattieri et al., 2014). At the contrary, the Gitana Cave speleothem records a strong moisture deficit, supporting a stronger impact of HS11 in the SW Mediterranean compared to the Italian Peninsula.

Finally, it is to be pointed out that HS12, occurring around 140 ka BP (Lisiecki & Stern, 2016), apparently did not have any imprint on the vegetation record of ODP 976, implying a subdued impact of this event on Mediterranean vegetation compared to HS11.

# 5.5. Comparison of MIS 6 with the last glacial period (MIS 4-2)

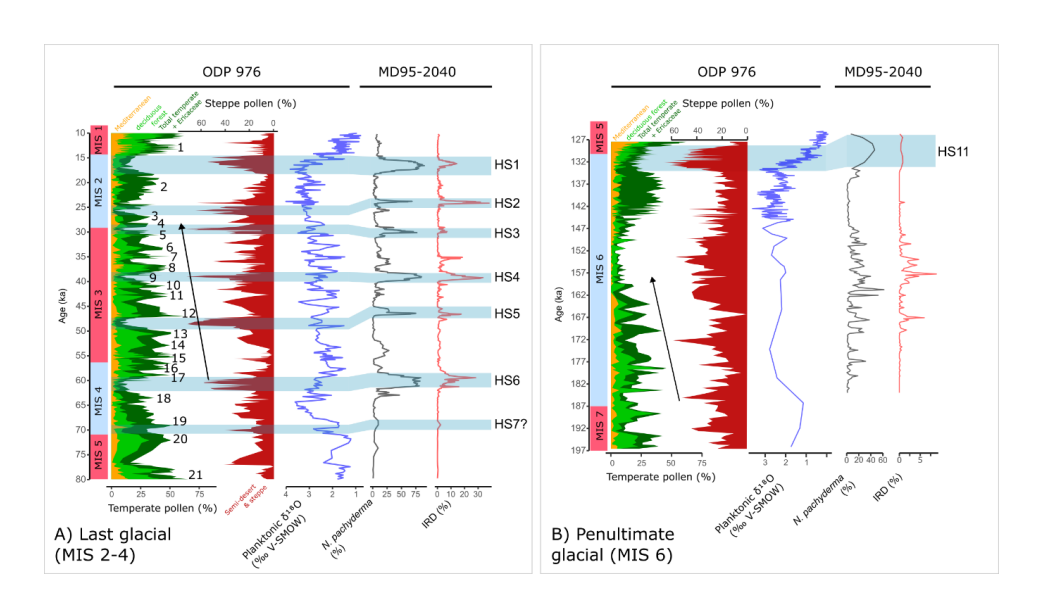






Fig. 9: Comparison of millennial changes during **A)** the last glacial (MIS 2-4) and **B)** The Penultimate glacial (MIS 6), including the main pollen data from ODP 976 (Charton et al., 2025; Combourieu-Nebout et al., 2002, 2009, and unpublished data for the last climatic cycle, and this study for MIS 6), the ODP 976 planktonic isotopic ratio from *G. bulloides* (Combourieu-Nebout et al., 2002; Jiménez-Amat & Zahn, 2015; von Grafenstein et al., 1999, and unpublished data), and the *N. pachyderma* and IRD record from core MD95-2040 (de Abreu et al., 2003). Marine Isotope Stages follow the boundaries from Lisiecki & Raymo (2005). Numbers on the Last Glacial correspond to the Greenland D-O events chronology (Fletcher et al., 2010; Rasmussen et al., 2014). Black arrows mark the aridification trend and decreasing interstadials intensity during MIS 3 and early MIS 6.

Various studies have pointed out strong similarities between the millennial-scale oscillations of the last glacial period and the penultimate glacial period, with the division between MIS 3 and MIS 2 being analogous to the early and mid-late phase of MIS 6 respectively (Held et al., 2024; Margari et al., 2010, 2014; Roucoux et al., 2011; Rousseau et al., 2020; Shin et al., 2020; Sierro et al., 2020). The same studies argued in favour of pervasive impact of stadial events on the continental climate and vegetation in the Mediterranean region, even in absence of typical Heinrich layers (Roucoux et al., 2011). The ODP 976 record shows a cooling and aridification trend during the first half of MIS 6 (Fig. 9), with decreasing intensity of interstadials events, that recalls the pattern of MIS 3 D-O cycles (Bond et al., 1993). However, the absence of clear successions of stadial events and especially Heinrich stadials, together with the more subdued expression of interstadials in the vegetation record, limits the resemblance between the two glacial periods. The pacing of interstadial peaks also seems to be reduced compared to the last glacial period high-frequency oscillations, as previously highlighted from the high-resolution speleothem record from Sofular cave in Turkey (Held et al., 2024).

 A comparison of millennial-scale changes during the past two glacial periods based on the ODP 976 and MD95-2040 records, on either side of the Gibraltar Strait, support our view (Fig. 9). The last glacial period (encompassing MIS 4 to MIS 2) was characterized in the Alboran Sea by high-intensity oscillations in both temperate and semi-desert vegetation correlated with D-O cycles and intense ice-rafting events HE1 to HE7 in MD95-2040. During interstadial events, temperate and Mediterranean vegetation (deciduous forest + Mediterranean + Ericaceae) could reach values above 60 % of total pollen; during stadial events, the semi-desert pollen values reached values as high as 70% of total pollen (during HS3, HS4 and HS5). In comparison, the penultimate glacial (MIS 6) displays much lower intensity events, with interstadials characterized by 45% as a maximum value for temperate vegetation, and stadials with 65% for the steppe and semi-desert vegetation (during HS11). High-intensity cold episodes during MIS 6 are limited to the HS11, and the ~172 ka BP event. This is consistent with the multiproxy record of core MD95-2040 on the Portuguese margin, which evidenced reduced variability in the *N. pachyderma* abundance and IRD deposition





during the penultimate glacial compared to the last glacial (de Abreu et al., 2003). The ice rafting episodes appear to be of different nature during MIS 6 (Hodell et al., 2008; Liu et al., 2018; McCarron et al., 2021), with the main iceberg discharges originating from the European ice sheet, contrary to the typical Hudson Strait origin of the last glacial Heinrich events. SST reconstructions in the western Mediterranean also show less intense cooling during MIS 6 than during MIS 3 (Martrat et al., 2004, 2007), supporting limited incursions of polar waters in the Mediterranean during MIS 6 compared to MIS 3 coldest stadials, and especially Heinrich stadials (Cacho et al., 1999).

Like ODP 976, Ioannina records lower intensity arboreal pollen oscillations during early MIS 6 compared to the last glacial (Roucoux et al., 2011). In comparison, the Atlantic pollen record from MD01-2444 core displays similar amplitude of tree percentages during the last and the penultimate glacial (Margari et al., 2010). This difference can be explained by the different climate conditions, and the higher sensitivity to cold and aridity of sclerophyllous and deciduous forest vegetation on the Mediterranean side, as recorded in the ODP 976 and Ioannina palynological sequence. It appears that temperate vegetation in SW Mediterranean responded to millennial climate oscillations with higher intensity during the last glacial compared to the penultimate, probably because the climate in Europe was colder during MIS 6 compared to MIS 2. This is supported by larger European ice-sheet extension during the penultimate glacial (Ehlers et al., 2011; Ehlers and Gibbard, 2007b; Shackleton, 1987), favouring the long-term establishment of open landscapes mainly composed by steppe and semi-desert plants. The differences in humidity might not be as easily interpretable, with an early MIS 6 more humid, and a MIS 6 glacial maximum more arid, compared to MIS 3 and MIS 2 as also suggested by the Ioannina record (Roucoux et al., 2011). Future climate reconstructions applied to the complete last glacial cycle in ODP 976 and other Mediterranean long pollen sequences will help understanding the different climate configurations between the last two glacial periods.

## 5.6. Human occupation during MIS 6 in SW Europe

Only a limited number of sites in South-Western Europe have yielded archaeological layers attributed to MIS 6, and even fewer of them have been radiometrically dated allowing for a robust comparison with the environmental changes during MIS 6 (Fig. 10, supplementary table S2). The environmental proxies available in the archaeological layers (pollen, charcoal, macro and microfauna) can help the chronological attribution, but are often insufficient to establish a precise correlation with the high-resolution chrono-environmental framework of marine and glacial archives. Even when absolute dates are available, their large uncertainty range makes it difficult to correlate the human occupation phases with a specific substage of MIS 6. It is generally accepted that the northern part of Europe was almost completely depopulated during

https://doi.org/10.5194/egusphere-2025-5024 Preprint. Discussion started: 21 October 2025 © Author(s) 2025. CC BY 4.0 License.



797

798

799

800

801

802

803 804

805

806

807

808

809 810

811

812



MIS 6, with very few sites identified compared to the southern European fringes, indicating discontinuous occupation during more favourable climatic episodes (Hérisson et al., 2016) or total abandonment like in the British lands (Scott, 2011; Shaw et al., 2016; White and Pettitt, 2011). Southern France, Italy and the Iberian Peninsula could have represented climate refugia during the most extreme ice-cap advances (Bicho and Carvalho, 2022). Notably, Italy is particularly deprived of sites well-dated to MIS 6 including the isolated Neanderthal of Altamura, the short episode of elephant scavenging at Poggetti Vecchi, and the long sequence of San Bernardino cave which chronological range extends up to ~154 ka BP, a period marked by the most extensive glacial conditions of MIS 6. Some other few archaeological layers have been attributed to MIS 6, but they lack a robust chronological attribution (Aureli & Ronchitelli, 2018; Fontana et al., 2010, Fig. 10). One can hypothesise that regional climate conditions in the peninsula were particularly harsh after 150 ka, and that potential refugia sites remain to be identified in Italy. Palaeoecological reconstructions at the Poggetti Vecchi site indicated cold and dry open environment (Aranguren et al., 2019; Benvenuti et al., 2017). Interestingly, the chronological range for the site could coincide with a major stadial event at 171 ka BP identified in the ODP 976 core, and particularly well expressed in the Valle di Castiglione record (Fig. 6).

813

814





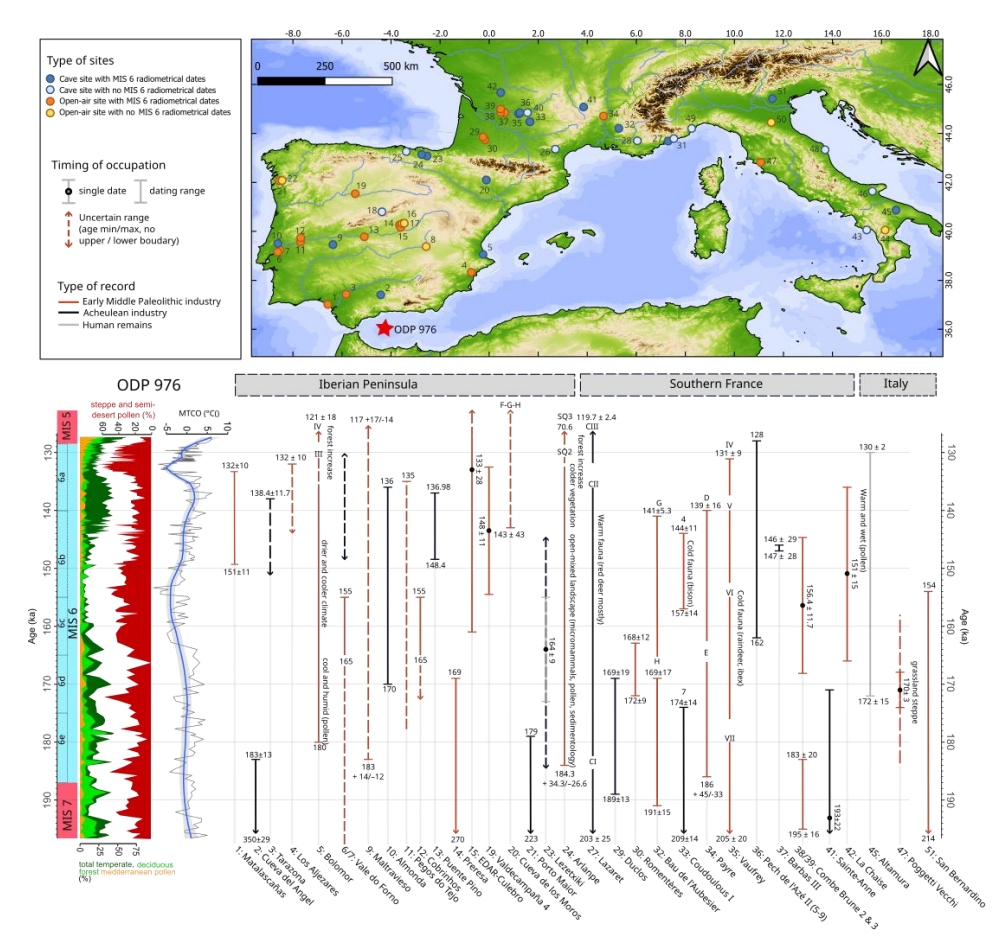


Fig. 10: Distribution of archaeological sites and radiometrically dated human occupation in western Mediterranean attributed to MIS 6, with some relevant palaeoecological information when available. The dates used and references can be found in Supplementary table S2. Sites on the map are numbered from south to north in each country: 1: Matalascañas; 2: Cueva del Angel; 3: Tarazona; 4: Los Aljezares; 5: Cueva del Bolomor; 6: Vale do Forno; 7: VF3 (Milharos); 8: El Provencio; 9: Cueva de Maltravieso; 10: Almonda; 11: Pegos do Tejo; 12: Cobrinhos; 13: Puente Pino; 14: Preresa; 15: EDAR-Culebro 2; 16: Arriaga II/III; 17: Arganda II (Valdocarros); 18: Villacastin; 19: Valdecampana; 20: Cueva de los Moros de Gabasa; 21: Porto Maior; 22: Arbo; 23: Lezetxiki; 24: Arlanpe; 25: Ventalaperra; 26: Aldènes; 27: Grotte du Lazaret; 28: Baume Bonne; 29: Duclos; 30: Romenteres; 31: Grotte du Prince; 32: Bau de l'Aubesier; 33: Coudoulous I; 34: Payre; 35: Grotte Vaufrey; 36: Pech de l'Aze II; 37: Barbas III; 38: Combe Brune 3; 39: Combe Brune 2; 40: Grotte Sirogne; 41: Sainte -Anne; 42: La Chaise; 43: Riparo del Poggio; 44: Rosaneto; 45: Altamura; 46: Riparo Paglicci; 47: Poggetti Vecchi; 48: Monte Conero; 49: Grotta del Colombo; 50: Due Pozzi/Scornetta; 51: Grotta di San Bernardino.

817

818

In Southern France and the Iberian Peninsula, according to available radiometric dates, human occupation appears to have been continuous across MIS 6, even during the glacial

https://doi.org/10.5194/egusphere-2025-5024 Preprint. Discussion started: 21 October 2025 © Author(s) 2025. CC BY 4.0 License.



819

820

821

822

823

824

825

826 827

828 829

830

831

832

833

834

835

836

837

838 839

840

841

842

843 844

845

846

847

848

849

850

851

852

853

854



maximum, with both cave and open-air sites. France provides a comparable number of cave and open-air sites mainly concentrated in the southwestern region. The Portuguese record is mainly constituted by open-air sites in fluvial terrace systems of the lower Tagus, offering important insights into short-term occupations during the full-glacial stage, but with complex chronological attribution (Cunha et al., 2012, 2017; Pereira et al., 2019). The Spanish record includes various open-air settlements in the upper Tagus valley (Panera et al., 2011, 2014; Yravedra et al., 2019), as well as the Duero (Diez-Martín, 2010) and the Guadalquivir (Caro Gómez et al., 2011) valleys. Cave sites are fewer and are mainly located closer to the coast (Cueva del Bolomor, Cueva del Angel, Lezetxiki, Arlanpe, Ventalaperra), with the two exceptions of Cueva de Maltravieso and Villacastín. Key sites like Lazaret cave (Late Acheulean, France) and Cueva del Bolomor (Middle Palaeolithic, Spain) evidence the persistence of human groups in possible climate refugia where large game hunting of red deer was prevailed (Michel et al., 2013; Valensi et al., 2013). Cueva del Bolomor stands out in the Iberian Peninsula record as it provides an exceptionally long and continuous record of human presence, and the oldest evidence of fire use in Spain during the Middle Palaeolithic (Vidal-Matutano et al., 2019). Climate changes during MIS 6 are documented in the cave's sediments through multiple proxies, with a more humid and cool phase at the beginning, and the most arid phase taking place at the middle of Phase III (layers X-VIII) (Arsuaga et al., 2012; Fernández Peris et al., 2008). The site is described as a climate refugia where Mediterranean vegetation persisted during the colder phase of MIS 6 thanks to the coastal reservoir character of the site (Ochando et al., 2019).

MIS 6 in Europe saw the final stage of the cultural transition from the Lower to the Middle Palaeolithic industries (MIS 8-5), mainly characterized by the emergence of more complex core technologies such as Levallois debitage and changes in subsistence strategies. No rupture is observed between the technocomplexes, as cultural diversity and the permanence of Acheulean bifacial tools associated to technological innovation mark these Early Middle Palaeolithic industries in Southern Europe (Santonja et al., 2016; Terradillos-Bernal et al., 2023). The distribution of archaeological sites and timing of human occupation in South-Western Mediterranean at that time reflects this pattern. A mosaic of traditional and innovative behavioural traits can be observed, with Acheulean and Early Middle Palaeolithic coexisting continuously (Cueto et al., 2016; de Lumley, 2018; Mathias et al., 2020; Moncel et al., 2025; Santonja et al., 2022; Torres et al., 2024; Valensi et al., 2013). Acheulean technocomplexes are progressively abandoned across MIS 6 in Europe (Álvarez-Alonso, 2014; Key et al., 2021), with the latest chronologies found possibly in the Manzanares basin in central Iberia at Arriaga sites (Panera et al., 2014; Rubio-Jara et al., 2016; Rubio-Jara and Panera, 2019; Silva et al., 2013), or at Lazaret cave (Michel et al., 2022), and dated to the beginning of MIS 5. No clear



855

856

857 858

859

860 861

862863

864

865

866

867

868 869

870

871

872

873

874

875

876

877

878

879 880

881

882

883

884

885

886

887

888 889

890



explanation is accepted for the emergence of the Levallois debitage, and while cognition might not be the only factor, some authors suggested that MIS 6 glaciation could have played a role in the final abandonment of Acheulean industries (Moncel et al., 2020; Valensi et al., 2005). Changes in land use and mobility pattern have been evidenced in north-central Iberia, and can be viewed as adaptations to the severe climatic conditions of MIS 6: increasing mobility, more short-term occupations and reliance on more local resources for subsistence strategies (Diez-Martín, 2010; Diez-Martín et al., 2008; Rios-Garaizar, 2016; Sánchez-Yustos, 2009). According to this view, the emergence of the "classical Neanderthal" world in Europe after the MIS 6/5 transition corresponds to the initialization of dynamics of repeated population contraction and expansion in response to the Upper Pleistocene instability (Sánchez-Yustos, 2009).

Indeed, the fast climate dynamics during Termination II as evidenced in the ODP 976 paleoenvironmental record could have represented a critical period for human population. At the end of MIS 6, more sites have been identified in the Iberian Peninsula than Southern France, showing the latter could have represented a climate refugia at the time of maximum glacial expansion, with more intense human occupation regionally. Many of these late MIS 6 sites present a chronological boundary at the top of the sequence compatible with the onset of Termination II around 136 ka BP, and with Heinrich Stadial 11, within the dating uncertainty: Matalascañas, Tarrazona, Los Aljezares, Bolomor Unit III, Almonda, Pegos do Tejo, Puente Pino, Arlanpe Unit SQ2, Lazaret Unit CII, Payre layer D, Vauffrey unit IV, and Pech de l'Azé II layer 5. The extreme character of this event in the South-Western Mediterranean as expressed in the ODP 976 sequence could have put further environmental pressure on hominin groups already diminished. The niche space reconstructed for Neanderthals at the end of MIS 6 (~145ka BP) is very reduced, and concentrated in Western Europe (Yaworsky et al., 2024). A regional study focused on North-Western Spain also argued in favour of a demographic vacuum at the end of MIS 6 leading to a population reorganization implying population retreat or micro-extinction, before the generalization of Middle Palaeolithic industries and during MIS 5 (Sánchez-Yustos and Diez-Martín, 2015). According to the same authors, following this crisis, Neanderthal population entered a "reorganisation phase" leading to demographical stability (Peyrégne et al., 2019) and more technological standardization, visible in the explosion of the number of sites in Europe in general, especially after the MIS 5e climatic optimum (Bringmans, 2007; Lewis et al., 2011; Wenzel, 2007). Thus, HS11 did not lead to complete extinction of hominin groups but might have induced deep demographical and technological reorganization, representing the first and one of the most intense abrupt changes that Neanderthal population had to face in South-Western Europe before the Last Glacial largest oscillations (HS4-6).





891

#### 6. Conclusion

892893894

895

896

897

898

899

900

901

902

903

904

905

906

907

908

909

910

911 912

913

914

915

916

917

918

919 920

921 922

923

924 925

The ODP 976 record shed light on the environmental and climate changes during MIS 6 in the SW Mediterranean. The sequence is characterized by the high representation of Cedrus and Ericaceae pollen, resulting from the combined influence of African and Atlantic input respectively. ODP 976 position, at the confluence of Mediterranean versus Atlantic, and Eurasian versus African climatic areas, is ideal to decipher the processes behind orbital and sub-orbital climate dynamics during past glaciations. Three main phases have been distinguished during MIS 6 with different trends in vegetation and climate changes. Millennialscale oscillations are recorded especially during the early part of MIS 6 (~187-166 ka BP) through the rapid increases of temperate and Mediterranean pollen, some of which are consistent with Antarctic and D-O-like events identified in the ice-core and marine temperature records, and other palynological sequences in the Mediterranean region. This Early MIS 6 phase is characterized by overall warmer and wetter climate conditions, in agreement with other paleoclimate archives in the Mediterranean showing enhanced moisture availability at the beginning of MIS 6. This phase of enhanced moisture availability was likely connected with enhanced Asian and African monsoon activity and was probably at the origin of the deposition of an Organic Rich Layer in the Alboran Sea and sapropel S6 in the eastern Mediterranean. The second phase (165-144 ka BP) shows the establishment of full glacial conditions in the Mediterranean, with the maximum spread of steppe and semi-desert vegetation associated to cold and arid climate conditions and limited rapid oscillations. Finally, the final stages of MIS 6 are marked by increased humidity and the development of Ericaceae, with moderate millennial-scale oscillations seen in the vegetation record. Termination II is very particular in the ODP 976 record, with the continuous increase of temperate and Mediterranean vegetation being contemporaneous to a major episode of steppe expansion and aridity increase identified as Heinrich Stadial 11. This event shows a particular three phases or "double u" shape, in agreement with other records, and probably had a major impact on the SW Mediterranean region. A comparison with the changes occurring during the last glacial period (MIS 2-4) inferred from the same core highlighted the limited duration, frequency and intensity of MIS 6 millennial climate events compared the last Glacial D-O cycles and Heinrich Events (MIS 2-4). These results support a subdued impact of the millennial-scale climate oscillations on the continental vegetation in the Mediterranean region during the Penultimate glaciation compared to the Last Glacial. The only exception is HS11, which stands out by its notable intensity and duration and is of particular interest to understand the mechanisms behind Termination II.





Human population continuously inhabited the SW Mediterranean territory during MIS 6. While few sites are available and robustly dated to MIS 6 in Italy, Southern France and the Iberian Peninsula appear to have been intensely populated, supporting their nature of Pleistocene Climate refugia. More ecological data from well-dated archaeological sites during MIS 6 would be needed to increase the quality of human-environmental dynamics comparison. However, the synthesis drawn in the present study highlights the extreme nature of events characterizing Termination II, and particularly HS11, which could have represented an important environmental crisis for human population at that time, catalysing the end of the Lower to Middle Palaeolithic Transition through a drastic population contraction.

## 7. Author contribution

LC, NC, AB and VL designed the project. LC and NC carried out the palynological analyses.

938 LC, OP and MR applied the four methods of pollen-based climate reconstruction to the ODP

976 record. LC and MHM led the archaeological synthesis. LC made the figures and wrote the

940 text. All authors contributed to improve the manuscript by their expertise.

### 8. Competing interests

Odile Peyron is a member of the editorial board of CP

# 9. Acknowledgments

We acknowledge the International Ocean Drilling Project and the MARUM Bremen Core Repository for making available the ODP 976 samples. The sample processing was funded by the CNRS and the MNHN. We thank the European Research Council (ERC) under the European Union's HORIZON1.1 research program (LATEUROPE project, grant agreement ID 101052653) for funding. L. Charton doctoral contract is funded by the French Ministère de l'Enseignement Supérieur et de la Recherche at the doctoral school ED 227 of the Muséum National d'Histoire Naturelle, Paris. The international co-tutorship with the University of Florence is supported by the Ecole Franco-Italienne Vinci grant (project C2-166). We thank Lionel Dubost for assistance in laboratory treatment of samples to HF. We are grateful to Francisco Sierro for sharing the isotopic data on AICC2012 timescale, to Jon Camuera for the pollen data from Padul and to Katherine Roucoux for the pollen data from Ioannina. Artificial Intelligence was used occasionally to improve the quality of English writing, as well as the performance of R codes. This is an ISEM contribution Number XXXX.

### 10. Data availability





- 961 Pollen counts and climate reconstruction results from ODP 976 will soon be submitted to PANGAEA
- 962 data repository (<a href="https://www.pangaea.de/">https://www.pangaea.de/</a>).

### 963 11. Supplement link

964

- 965 The supplement link includes:
- 966 S1: ERA 5 extraction of the modern climate parameters for ODP 976.
- 967 S2 : Table of archaeological sites and dates used for the synthesis of human occupation in
- 968 western Mediterranean Europe during MIS 6.

## 969 12. References

970

- 971 de Abreu, L., Shackleton, N. J., Schönfeld, J., Hall, M., and Chapman, M.: Millennial-scale
- 972 oceanic climate variability off the Western Iberian margin during the last two glacial periods,
- 973 Marine Geology, 196, 1–20, https://doi.org/10.1016/S0025-3227(03)00046-X, 2003.
- 974 Allen, J. R. M. and Huntley, B.: Last Interglacial palaeovegetation, palaeoenvironments and
- 975 chronology: a new record from Lago Grande di Monticchio, southern Italy, Quaternary Science
- 976 Reviews, 28, 1521–1538, https://doi.org/10.1016/j.quascirev.2009.02.013, 2009.
- 977 Álvarez-Alonso, D.: First Neanderthal settlements in northern Iberia: The Acheulean and the
- 978 emergence of Mousterian technology in the Cantabrian region, Quaternary International, 326–
- 979 327, 288–306, https://doi.org/10.1016/j.quaint.2012.12.023, 2014.
- Aranguren, B., Grimaldi, S., Benvenuti, M., Capalbo, C., Cavanna, F., Cavulli, F., Ciani, F.,
- 981 Comencini, G., Giuliani, C., Grandinetti, G., Mariotti Lippi, M., Masini, F., Mazza, P. P. A.,
- 982 Pallecchi, P., Santaniello, F., Savorelli, A., and Revedin, A.: Poggetti Vecchi (Tuscany, Italy):
- 983 A late Middle Pleistocene case of human-elephant interaction, Journal of Human Evolution,
- 984 133, 32–60, https://doi.org/10.1016/j.jhevol.2019.05.013, 2019.
- 985 Arsuaga, J. L., Fernández Peris, J., Gracia-Téllez, A., Quam, R., Carretero, J. M., Barciela
- 986 González, V., Blasco, R., Cuartero, F., and Sañudo, P.: Fossil human remains from Bolomor
- 987 Cave (Valencia, Spain), Journal of Human Evolution, 62, 629-639,
- 988 https://doi.org/10.1016/j.jhevol.2012.02.002, 2012.
- 989 Auffret, G.-A., Pastouret, L., Chamley, H., and Lanoix, F.: Influence of the prevailing current
- 990 regime on sedimentation in the Alboran Sea, Deep Sea Research and Oceanographic
- 991 Abstracts, 21, 839–849, https://doi.org/10.1016/0011-7471(74)90003-5, 1974.
- 992 Aureli, D. and Ronchitelli, A.: The Lower Tyrrhenian Versant: was it a techno-cultural area
- 993 during the Middle Palaeolithic? Evolution of the lithic industries of the Riparo del Molare
- sequence in the frame of Neanderthal peopling dynamics in Italy, 59–94, 2018.
- 995 Ayalon, A., Bar-Matthews, M., and Kaufman, A.: Climatic conditions during marine oxygen
- 996 isotope stage 6 in the eastern Mediterranean region from the isotopic composition of
- 997 speleothems of Soreq Cave, Israel, Geology, 30, https://doi.org/10.1130/0091-
- 998 7613(2002)030<0303:CCDMOI>2.0.CO;2, 2002.
- 999 Bailey, G., Carrión, J., Fa, D., Finlayson, C., Finlayson, G., and Vidal, J.: The coastal shelf of
- 1000 the Mediterranean and beyond: Corridor and refugium for human populations in the





- 1001 Pleistocene Introduction, Quaternary Science Reviews, 27, 2095–2099,
- 1002 https://doi.org/10.1016/j.quascirev.2008.08.005, 2008.
- 1003 Bajo, P., Drysdale, R. N., Woodhead, J. D., Hellstrom, J. C., Hodell, D., Ferretti, P., Voelker,
- 1004 A. H. L., Zanchetta, G., Rodrigues, T., Wolff, E., Tyler, J., Frisia, S., Spötl, C., and Fallick, A.
- 1005 E.: Persistent influence of obliquity on ice age terminations since the Middle Pleistocene
- transition, Science, 367, 1235–1239, https://doi.org/10.1126/science.aaw1114, 2020.
- 1007 Barbante, C., Barnola, J.-M., Becagli, S., Beer, J., Bigler, M., Boutron, C., Blunier, T.,
- 1008 Castellano, E., Cattani, O., Chappellaz, J., Dahl-Jensen, D., Debret, M., Delmonte, B., Dick,
- D., Falourd, S., Faria, S., Federer, U., Fischer, H., Freitag, J., Frenzel, A., Fritzsche, D., Fundel,
- 1010 F., Gabrielli, P., Gaspari, V., Gersonde, R., Graf, W., Grigoriev, D., Hamann, I., Hansson, M.,
- 1011 Hoffmann, G., Hutterli, M. A., Huybrechts, P., Isaksson, E., Johnsen, S., Jouzel, J.,
- 1012 Kaczmarska, M., Karlin, T., Kaufmann, P., Kipfstuhl, S., Kohno, M., Lambert, F., Lambrecht,
- A., Lambrecht, A., Landais, A., Lawer, G., Leuenberger, M., Littot, G., Loulergue, L., Lüthi, D.,
- Maggi, V., Marino, F., Masson-Delmotte, V., Meyer, H., Miller, H., Mulvaney, R., Narcisi, B.,
- Oerlemans, J., Oerter, H., Parrenin, F., Petit, J.-R., Raisbeck, G., Raynaud, D., Röthlisberger,
- 1016 R., Ruth, U., Rybak, O., Severi, M., Schmitt, J., Schwander, J., Siegenthaler, U., Siggaard-
- 1017 Andersen, M.-L., Spahni, R., Steffensen, J. P., Stenni, B., Stocker, T. F., Tison, J.-L., Traversi,
- 1018 R., Udisti, R., Valero-Delgado, F., van den Broeke, M. R., van de Wal, R. S. W., Wagenbach,
- D., Wegner, A., Weiler, K., Wilhelms, F., Winther, J.-G., Wolff, E., and EPICA Community
- 1020 Members: One-to-one coupling of glacial climate variability in Greenland and Antarctica,
- 1021 Nature, 444, 195–198, https://doi.org/10.1038/nature05301, 2006.
- 1022 Bard, E., Delaygue, G., Rostek, F., Antonioli, F., Silenzi, S., and Schrag, D. P.: Hydrological
- 1023 conditions over the western Mediterranean basin during the deposition of the cold Sapropel 6
- 1024 (ca. 175 kyr BP), Earth and Planetary Science Letters, 202, 481-494,
- 1025 https://doi.org/10.1016/S0012-821X(02)00788-4, 2002.
- Barker, S. and Knorr, G.: Millennial scale feedbacks determine the shape and rapidity of glacial
- termination, Nat Commun, 12, 2273, https://doi.org/10.1038/s41467-021-22388-6, 2021.
- Barker, S., Knorr, G., Edwards, R. L., Parrenin, F., Putnam, A. E., Skinner, L. C., Wolff, E., and
- 1029 Ziegler, M.: 800,000 Years of Abrupt Climate Variability, Science, 334, 347-351,
- 1030 https://doi.org/10.1126/science.1203580, 2011.
- 1031 Bazin, L., Landais, A., Lemieux-Dudon, B., Toyé Mahamadou Kele, H., Veres, D., Parrenin,
- 1032 F., Martinerie, P., Ritz, C., Capron, E., Lipenkov, V., Loutre, M.-F., Raynaud, D., Vinther, B.,
- 1033 Svensson, A., Rasmussen, S. O., Severi, M., Blunier, T., Leuenberger, M., Fischer, H.,
- 1034 Masson-Delmotte, V., Chappellaz, J., and Wolff, E.: An optimized multi-proxy, multi-site
- Antarctic ice and gas orbital chronology (AICC2012): 120–800 ka, Climate of the Past,
- 1036 9, 1715–1731, https://doi.org/10.5194/cp-9-1715-2013, 2013.
- 1037 Benvenuti, M., Bahain, J.-J., Capalbo, C., Capretti, C., Ciani, F., D'Amico, C., Esu, D., Giachi,
- 1038 Gi., Giuliani, C., Gliozzi, E., Lazzeri, S., Macchioni, N., Lippi, M. M., Masini, F., Mazza, P. P.
- 1039 A., Pallecchi, P., Revedin, A., Savorelli, A., Spadi, M., Sozzi, L., Vietti, A., Voltaggio, M., and
- 1040 Aranguren, B.: Paleoenvironmental context of the early Neanderthals of Poggetti Vecchi for
- 1041 the late middle Pleistocene of Central Italy, Quat. res., 88, 327-344,
- 1042 https://doi.org/10.1017/qua.2017.51, 2017.
- 1043 Bermúdez de Castro, J. M. and Martinón-Torres, M.: A new model for the evolution of the
- human Pleistocene populations of Europe, Quaternary International, 295, 102-112,
- 1045 https://doi.org/10.1016/j.quaint.2012.02.036, 2013.





- 1046 Bicho, N. and Carvalho, M.: Peninsular southern Europe refugia during the Middle Palaeolithic:
- an introduction, J Quaternary Science, 37, 133–135, https://doi.org/10.1002/jqs.3410, 2022.
- 1048 Bisschop, K., Mortier, F., Etienne, R. S., and Bonte, D.: Transient local adaptation and source-
- 1049 sink dynamics in experimental populations experiencing spatially heterogeneous
- 1050 environments, Proceedings of the Royal Society B: Biological Sciences, 286, 20190738,
- 1051 https://doi.org/10.1098/rspb.2019.0738, 2019.
- Bond, G., Heinrich, H., Broecker, W., Labeyrie, L., McManus, J., Andrews, J., Huon, S.,
- 1053 Jantschik, R., Clasen, S., Simet, C., Tedesco, K., Klas, M., Bonani, G., and Ivy, S.: Evidence
- for massive discharges of icebergs into the North Atlantic ocean during the last glacial period,
- 1055 Nature, 360, 245–249, https://doi.org/10.1038/360245a0, 1992.
- 1056 Bond, G., Broecker, W., Johnsen, S., McManus, J., Labeyrie, L., Jouzel, J., and Bonani, G.:
- 1057 Correlations between climate records from North Atlantic sediments and Greenland ice,
- 1058 Nature, 365, 143–147, https://doi.org/10.1038/365143a0, 1993.
- Bond, G., Showers, W., Cheseby, M., Lotti, R., Almasi, P., Demenocal, P., Priore, P., Cullen,
- 1060 H., Hajdas, I., and Bonani, G.: A pervasive millennial-scale cycle in the North Atlantic Holocene
- and glacial climates, sci, 278, 1257, https://doi.org/10.1126/science.278.5341.1257, 1997.
- Bond, G. C., Showers, W., Elliot, M., Evans, M., Lotti, R., Hajdas, I., Bonani, G., and Johnson,
- 1063 S.: The North Atlantic's 1-2 kyr climate rhythm: Relation to Heinrich events,
- 1064 Dansgaard/Oeschger cycles and the Little Ice Age, Washington DC American Geophysical
- 1065 Union Geophysical Monograph Series, 112, 35-58, https://doi.org/10.1029/GM112p0035,
- 1066 1999.
- Boswell, S. M., Toucanne, S., Pitel-Roudaut, M., Creyts, T. T., Eynaud, F., and Bayon, G.:
- 1068 Enhanced surface melting of the Fennoscandian Ice Sheet during periods of North Atlantic
- 1069 cooling, Geology, 47, 664–668, https://doi.org/10.1130/G46370.1, 2019.
- 1070 Bout-Roumazeilles, V., Combourieu Nebout, N., Peyron, O., Cortijo, E., Landais, A., and
- 1071 Masson-Delmotte, V.: Connection between South Mediterranean climate and North African
- 1072 atmospheric circulation during the last 50,000yrBP North Atlantic cold events, Quaternary
- 1073 Science Reviews, 26, 3197–3215, https://doi.org/10.1016/j.quascirev.2007.07.015, 2007.
- 1074 ter Braak, C. and Juggins, S.: Weighted Averaging Partial Least Squares Regression (WA-
- 1075 PLS): An Improved Method for Reconstructing Environmental Variables from Species
- 1076 Assemblages, Hydrobiologia, 269–270, 485–502, https://doi.org/10.1007/BF00028046, 1993.
- 1077 Bradtmöller, M., Pastoors, A., Weninger, B., and Weniger, G.-C.: The repeated replacement
- 1078 model Rapid climate change and population dynamics in Late Pleistocene Europe,
- 1079 Quaternary International, 247, 38–49, https://doi.org/10.1016/j.quaint.2010.10.015, 2012.
- 1080 Brauer, A., Allen, J. R. M., Mingram, J., Dulski, P., Wulf, S., and Huntley, B.: Evidence for last
- interglacial chronology and environmental change from Southern Europe, Proceedings of the
- 1082 National Academy of Sciences, 104, 450-455, https://doi.org/10.1073/pnas.0603321104,
- 1083 2007.
- 1084 Bringmans, P.: First Evidence of Neanderthal Presence in Northwest Europe during the Late
- 1085 Saalian "Zeifen Interstadial" (MIS 6.01) found at the VLL and VLB Sites at Veldwezelt-
- Hezerwater, Belgium, Journal of Archaeology of Northwest Europe, 1, 2007.





- Broecker, W. S. and Henderson, G. M.: The sequence of events surrounding Termination II
- and their implications for the cause of glacial-interglacial CO2 changes, Paleoceanography,
- 1089 13, 352–364, 1998.
- 1090 Burns, S. J., Welsh, L. K., Scroxton, N., Cheng, H., and Edwards, R. L.: Millennial and orbital
- scale variability of the South American Monsoon during the penultimate glacial period, Sci Rep,
- 9, 1234, https://doi.org/10.1038/s41598-018-37854-3, 2019.
- 1093 Cacho, I., Grimalt, J. O., Pelejero, C., Canals, M., Sierro, F. J., Flores, J. A., and Shackleton,
- 1094 N.: Dansgaard-Oeschger and Heinrich event imprints in Alboran Sea paleotemperatures,
- 1095 Paleoceanography, 14, 698–705, https://doi.org/10.1029/1999PA900044, 1999.
- 1096 Cacho, I., Shackleton, N., Elderfield, H., Sierro, F. J., and Grimalt, J. O.: Glacial rapid variability
- 1097 in deep-water temperature and δ18O from the Western Mediterranean Sea, Quaternary
- 1098 Science Reviews, 25, 3294–3311, https://doi.org/10.1016/j.guascirev.2006.10.004, 2006.
- 1099 Camuera, J., Jiménez-Moreno, G., Ramos-Román, M. J., García-Alix, A., Toney, J. L.,
- 1100 Anderson, R. S., Jiménez-Espejo, F., Bright, J., Webster, C., Yanes, Y., and Carrión, J. S.:
- 1101 Vegetation and climate changes during the last two glacial-interglacial cycles in the western
- 1102 Mediterranean: A new long pollen record from Padul (southern Iberian Peninsula), Quaternary
- 1103 Science Reviews, 205, 86–105, https://doi.org/10.1016/j.quascirev.2018.12.013, 2019.
- 1104 Camuera, J., Ramos-Román, M. J., Jiménez-Moreno, G., García-Alix, A., Ilvonen, L., Ruha,
- 1105 L., Gil-Romera, G., González-Sampériz, P., and Seppä, H.: Past 200 kyr hydroclimate
- 1106 variability in the western Mediterranean and its connection to the African Humid Periods, Sci
- 1107 Rep, 12, 9050, https://doi.org/10.1038/s41598-022-12047-1, 2022.
- 1108 Caro Gómez, J. A., Díaz Del Olmo, F., Artigas, R. C., Recio Espejo, J. M., and Barrera, C. B.:
- 1109 Geoarchaeological alluvial terrace system in Tarazona: Chronostratigraphical transition of
- 1110 Mode 2 to Mode 3 during the middle-upper pleistocene in the Guadalquivir River valley (Seville,
- 1111 Spain), Quaternary International, 243, 143–160, https://doi.org/10.1016/j.quaint.2011.04.022,
- 1112 2011.
- 1113 Chapman, M. R. and Shackleton, N. J.: Global ice-volume fluctuations, North Atlantic ice-
- rafting events, and deep-ocean circulation changes between 130 and 70 ka, Geology, 27, 795,
- 1115 https://doi.org/10.1130/0091-7613(1999)027<0795:GIVFNA>2.3.CO;2, 1999.
- 1116 Chappellaz, J., Brook, E., Blunier, T., and Malaizé, B.: CH<sub>4</sub> and  $\delta^{18}$  O of O<sub>2</sub> records from
- 1117 Antarctic and Greenland ice: A clue for stratigraphic disturbance in the bottom part of the
- 1118 Greenland Ice Core Project and the Greenland Ice Sheet Project 2 ice cores, J. Geophys.
- 1119 Res., 102, 26547–26557, https://doi.org/10.1029/97JC00164, 1997.
- 1120 Charton, L.: Vegetation and climate changes during the Middle to Upper Palaeolithic transition
- in the southwestern Mediterranean: What happened to the last Neanderthals during Heinrich
- stadial 4?, Quaternary Science Reviews, 2025.
- 1123 Charton, L., Combourieu-Nebout, N., Bertini, A., Lebreton, V., Peyron, O., Robles, M.,
- 1124 Sassoon, D., and Moncel, M.-H.: Vegetation and climate changes during the Middle to Upper
- 1125 Palaeolithic transition in the southwestern Mediterranean: What happened to the last
- 1126 Neanderthals during Heinrich stadial 4?, 2025.
- 1127 Cheddadi, R. and Rossignol-Strick, M.: Eastern Mediterranean Quaternary paleoclimates from
- pollen and isotope records of marine cores in the Nile Cone Area, Paleoceanography, 10, 291–
- 300, https://doi.org/10.1029/94PA02672, 1995.





- 1130 Cheng, H., Edwards, R. L., Wang, Y., Kong, X., Ming, Y., Kelly, M. J., Wang, X., Gallup, C. D.,
- and Liu, W.: A penultimate glacial monsoon record from Hulu Cave and two-phase glacial
- terminations, Geology, 34, 217–220, https://doi.org/10.1130/G22289.1, 2006.
- 1133 Chevalier, M., Davis, B. A. S., Heiri, O., Seppä, H., Chase, B. M., Gajewski, K., Lacourse, T.,
- Telford, R. J., Finsinger, W., Guiot, J., Kühl, N., Maezumi, S. Y., Tipton, J. R., Carter, V. A.,
- 1135 Brussel, T., Phelps, L. N., Dawson, A., Zanon, M., Vallé, F., Nolan, C., Mauri, A., de Vernal,
- 1136 A., Izumi, K., Holmström, L., Marsicek, J., Goring, S., Sommer, P. S., Chaput, M., and
- 1137 Kupriyanov, D.: Pollen-based climate reconstruction techniques for late Quaternary studies,
- 1138 Earth-Science Reviews, 210, https://doi.org/10.1016/j.earscirev.2020.103384, 2020.
- 1139 Colleoni, F., Wekerle, C., Näslund, J.-O., Brandefelt, J., and Masina, S.: Constraint on the
- 1140 penultimate glacial maximum Northern Hemisphere ice topography (≈140 kyrs BP),
- 1141 Quaternary Science Reviews, 137, 97–112, https://doi.org/10.1016/j.quascirev.2016.01.024,
- 1142 2016.
- 1143 Combourieu-Nebout, N., Turon, J. L., Zahn, R., Capotondi, L., Londeix, L., and Pahnke, K.:
- 1144 Enhanced aridity and atmospheric high-pressure stability over the western Mediterranean
- during the North Atlantic cold events of the past 50 k.y., Geol, 30, 863,
- 1146 https://doi.org/10.1130/0091-7613(2002)030<0863:EAAAHP>2.0.CO;2, 2002.
- 1147 Combourieu-Nebout, N., Peyron, O., Dormoy, I., Desprat, S., Célia, B., Kotthoff, U., and
- 1148 Marret, F.: Rapid climatic variability in the west Mediterranean during the last 25 000 years
- from high resolution pollen data, Climate of the Past, 5, https://doi.org/10.5194/cpd-5-671-
- 1150 2009, 2009.
- 1151 Cortina, A., Sierro, F. J., Flores, J. A., Martrat, B., and Grimalt, J. O.: The response of SST to
- insolation and ice sheet variability from MIS 3 to MIS 11 in the northwestern Mediterranean
- 1153 Sea (Gulf of Lions), Geophysical Research Letters, 42, 10,366-10,374,
- 1154 https://doi.org/10.1002/2015GL065539, 2015.
- 1155 Cueto, S., Preysler, J., Pérez-González, A., Torres, C., Pérez, I., and Miguel, J.: Acheulian flint
- 1156 quarries in the Madrid Tertiary basin, central Iberian Peninsula: First data obtained from
- 1157 geoarchaeological studies, Quaternary International, 411,
- 1158 https://doi.org/10.1016/j.quaint.2016.01.041, 2016.
- 1159 Cunha, P. P., Almeida, N. A. C., Aubry, T., Martins, A. A., Murray, A. S., Buylaert, J.-P.,
- 1160 Sohbati, R., Raposo, L., and Rocha, L.: Records of human occupation from Pleistocene river
- terrace and aeolian sediments in the Arneiro depression (Lower Tejo River, central eastern
- Portugal), Geomorphology, 165–166, 78–90, https://doi.org/10.1016/j.geomorph.2012.02.017,
- 1163 2012.
- 1164 Cunha, P. P., Martins, A. A., Buylaert, J.-P., Murray, A. S., Raposo, L., Mozzi, P., and Stokes,
- 1165 M.: New data on the chronology of the Vale do Forno sedimentary sequence (Lower Tejo River
- terrace staircase) and its relevance as a fluvial archive of the Middle Pleistocene in western
- 1167 Iberia, Quaternary Science Reviews, 166, 204–226,
- 1168 https://doi.org/10.1016/j.quascirev.2016.11.001, 2017.
- Dansgaard, W., Johnsen, S. J., Clausen, H. B., Dahl-Jensen, D., Gundestrup, N. S., Hammer,
- 1170 C. U., Hvidberg, C. S., Steffensen, J. P., Sveinbjörnsdottir, A. E., and Jouzel, J.: Evidence for
- general instability of past climate from a 250-kyr ice-core record, Nature, 364, 218–220, 1993.
- 1172 Davtian, N. and Bard, E.: A new view on abrupt climate changes and the bipolar seesaw based
- on paleotemperatures from Iberian Margin sediments, Proceedings of the National Academy
- 1174 of Sciences, 120, e2209558120, https://doi.org/10.1073/pnas.2209558120, 2023.





- 1175 Dennell, R. W., Martinón-Torres, M., and Bermúdez de Castro, J. M.: Hominin variability,
- 1176 climatic instability and population demography in Middle Pleistocene Europe, Quaternary
- 1177 Science Reviews, 30, 1511–1524, https://doi.org/10.1016/j.quascirev.2009.11.027, 2011.
- 1178 D'Errico, F. and Sánchez Goñi, M. F. S.: Neandertal extinction and the millennial scale climatic
- variability of OIS 3, Quaternary Science Reviews, 22, 769–788, https://doi.org/10.1016/S0277-
- 1180 3791(03)00009-X, 2003.
- 1181 Diez-Martín, F.: Evaluating the effect of plowing on the archaeological record: The early middle
- palaeolithic in the river Duero basin plateaus (north-central Spain), Quaternary International,
- 214, 30–43, https://doi.org/10.1016/j.quaint.2009.10.024, 2010.
- 1184 Diez-Martín, F., Sánchez-Yustos, P., Gómez-González, J. Á., and Gómez De La Rúa, D.:
- 1185 Earlier Palaeolithic Settlement Patterns: Landscape Archaeology on the River Duero Basin
- 1186 Plateaus (Castilla y León, Spain), J World Prehist, 21, 103-137
- 1187 https://doi.org/10.1007/s10963-008-9012-0, 2008.
- 1188 D'Oliveira, L., Dugerdil, L., Ménot, G., Evin, A., Muller, S., Ansanay-Alex, S., Azuara, J.,
- Bonnet, C., Bremond, L., Shah, M., and Peyron, O.: Reconstructing 15 000 years of southern
- 1190 France temperatures from coupled pollen and molecular (branched glycerol dialkyl glycerol
- tetraether) markers (Canroute, Massif Central), Climate of the Past, 19, 2127-2156,
- 1192 https://doi.org/10.5194/cp-19-2127-2023, 2023.
- 1193 Drysdale, R. N., Zanchetta, G., Hellstrom, J. C., Fallick, A. E., and Zhao, J.: Stalagmite
- evidence for the onset of the Last Interglacial in southern Europe at 129 ± 1 ka, Geophysical
- 1195 Research Letters, 32, https://doi.org/10.1029/2005GL024658, 2005.
- 1196 Dugerdil, L., Joannin, S., Peyron, O., Jouffroy-Bapicot, I., Vannière, B., Boldgiv, B., Unkelbach,
- 1197 J., Behling, H., and Ménot, G.: Climate reconstructions based on GDGT and pollen surface
- 1198 datasets from Mongolia and Baikal area: calibrations and applicability to extremely cold-dry
- 1199 environments over the Late Holocene, Climate of the Past, 17, 1199-1226,
- 1200 https://doi.org/10.5194/cp-17-1199-2021, 2021.
- 1201 Ehlers, J. and Gibbard, P. L.: The extent and chronology of Cenozoic Global Glaciation,
- 1202 Quaternary International, 164–165, 6–20, https://doi.org/10.1016/j.quaint.2006.10.008, 2007.
- 1203 Ehlers, J., Grube, A., Stephan, H.-J., and Wansa, S.: Pleistocene Glaciations of North
- 1204 Germany—New Results, in: Developments in Quaternary Sciences, vol. 15, Elsevier, 149-
- 1205 162, https://doi.org/10.1016/B978-0-444-53447-7.00013-1, 2011.
- 1206 Ehlers, J., Gibbard, P. L., and Hughes, P. D.: Chapter 4 Quaternary Glaciations and
- 1207 Chronology, in: Past Glacial Environments (Second Edition), edited by: Menzies, J. and van
- der Meer, J. J. M., Elsevier, 77–101, https://doi.org/10.1016/B978-0-08-100524-8.00003-8,
- 1209 2018.
- 1210 Emeis, K.-C., Schulz, H., Struck, U., Rossignol-Strick, M., Erlenkeuser, H., Howell, M. W.,
- 1211 Kroon, D., Mackensen, A., Ishizuka, S., Oba, T., Sakamoto, T., and Koizumi, I.: Eastern
- 1212 Mediterranean surface water temperatures and δ18O composition during deposition of
- 1213 sapropels in the late Quaternary, Paleoceanography, 18
- 1214 https://doi.org/10.1029/2000PA000617, 2003.
- 1215 Eynaud, F., Zaragosi, S., Scourse, J. D., Mojtahid, M., Bourillet, J. F., Hall, I. R., Penaud, A.,
- 1216 Locascio, M., and Reijonen, A.: Deglacial laminated facies on the NW European continental
- 1217 margin: The hydrographic significance of British-Irish Ice Sheet deglaciation and Fleuve





- 1218 Manche paleoriver discharges, Geochemistry, Geophysics, Geosystems, 8,
- 1219 https://doi.org/10.1029/2006GC001496, 2007.
- 1220 Faegri, K. and Iversen, J.: Textbook of Pollen Analysis, 4th Edition., John Wiley and Sons,
- 1221 Chichester, UK, 338 pp., 1964.
- 1222 Fernández Peris, J., Barciela, V., Blasco, R., Cuartero, F., and Sañudo, P.: El Paleolítico Medio
- 1223 en el territorio valenciano y la variabilidad tecno-económica de la Cova del Bolomor, Treballs
- 1224 d'Arqueologia, 141–169, 2008.
- 1225 Finlayson, C. and Carrión, J. S.: Rapid ecological turnover and its impact on Neanderthal and
- 1226 other human populations, Trends in Ecology & Evolution, 22, 213-222,
- 1227 https://doi.org/10.1016/j.tree.2007.02.001, 2007.
- 1228 Fletcher, W. J. and Sánchez Goñi, M. F.: Orbital- and sub-orbital-scale climate impacts on
- vegetation of the western Mediterranean basin over the last 48,000 yr, Quaternary Research,
- 1230 70, 451–464, https://doi.org/10.1016/j.yqres.2008.07.002, 2008.
- 1231 Fletcher, W. J., Sánchez Goñi, M. F., Allen, J. R. M., Cheddadi, R., Combourieu-Nebout, N.,
- 1232 Huntley, B., Lawson, I., Londeix, L., Magri, D., Margari, V., Müller, U. C., Naughton, F.,
- 1233 Novenko, E., Roucoux, K., and Tzedakis, P. C.: Millennial-scale variability during the last
- 1234 glacial in vegetation records from Europe, Quaternary Science Reviews, 29, 2839-2864,
- 1235 https://doi.org/10.1016/j.quascirev.2009.11.015, 2010.
- Foerster, V., Asrat, A., Bronk Ramsey, C., Brown, E. T., Chapot, M. S., Deino, A., Duesing,
- 1237 W., Grove, M., Hahn, A., Junginger, A., Kaboth-Bahr, S., Lane, C. S., Opitz, S., Noren, A.,
- 1238 Roberts, H. M., Stockhecke, M., Tiedemann, R., Vidal, C. M., Vogelsang, R., Cohen, A. S.,
- Lamb, H. F., Schaebitz, F., and Trauth, M. H.: Pleistocene climate variability in eastern Africa
- 1240 influenced hominin evolution, Nat Geosci, 15, 805–811, https://doi.org/10.1038/s41561-022-
- 1241 01032-y, 2022.
- 1242 Follieri, M., Magri, D., and Sadori, L.: A 250 000-years pollen record from Valle di Castiglione
- 1243 (Roma), Pollen et Spores, 30, 329-356, 1988.
- Fontana, F., Nenzioni, G., and Peretto, C.: The southern Po plain area (Italy) in the mid-late
- 1245 Pleistocene: Human occupation and technical behaviours, Quaternary International, 223, 465–
- 1246 471, https://doi.org/10.1016/j.quaint.2010.02.013, 2010.
- 1247 Gouzy, A., Malaizé, B., Pujol, C., and Charlier, K.: Climatic "pause" during Termination II
- 1248 identified in shallow and intermediate waters off the Iberian margin, Quaternary Science
- 1249 Reviews, 23, 1523–1528, https://doi.org/10.1016/j.quascirev.2004.03.002, 2004.
- von Grafenstein, R., Zahn, R., and Tiedemann, R.: Planktonic d18O records at Sites 976 and
- 977, Alboran Sea: stratigraphy, forcing, and paleoceanographic implications. In Curry, W.B.,
- Shackleton, N.J., and Richter, C, Proceedings Ocean Drilling Program Scientific Results, 154,
- 1253 299–318, 1999.
- 1254 Guiot, J.: Methodology of the last climatic cycle reconstruction in France from pollen data,
- 1255 Palaeogeography, Palaeoclimatology, Palaeoecology, 80, 49–69,
- 1256 https://doi.org/10.1016/0031-0182(90)90033-4, 1990.
- 1257 Guiot, J., Pons, A., De Beaulieu, J. L., and Reille, M.: A 140,000-year continental climate
- 1258 reconstruction from two European pollen records, Nature, 338, 309-313,
- 1259 https://doi.org/10.1038/338309a0, 1989.





- 1260 Guiot, J., De Beaulieu, J. L., Cheddadi, R., David, F., Ponel, P., and Reille, M.: The climate in
- 1261 Western Europe during the last Glacial/Interglacial cycle derived from pollen and insect
- 1262 remains, Palaeogeography, Palaeoclimatology, Palaeoecology, 103, 73–93,
- 1263 https://doi.org/10.1016/0031-0182(93)90053-L, 1993.
- 1264 Heinrich, H.: Origin and Consequences of Cyclic Ice Rafting in the Northeast Atlantic Ocean
- 1265 During the Past 130,000 Years, Quaternary Research, 29, 142-152,
- 1266 https://doi.org/10.1016/0033-5894(88)90057-9, 1988.
- 1267 Held, F., Cheng, H., Edwards, R. L., Tüysüz, O., Koç, K., and Fleitmann, D.: Dansgaard-
- 1268 Oeschger cycles of the penultimate and last glacial period recorded in stalagmites from
- 1269 Türkiye, Nat Commun, 15, 1183, https://doi.org/10.1038/s41467-024-45507-5, 2024.
- 1270 Hemming, S. R.: Heinrich events: Massive late Pleistocene detritus layers of the North Atlantic
- 1271 and their global climate imprint, Reviews of Geophysics, 42,
- 1272 https://doi.org/10.1029/2003RG000128, 2004.
- 1273 Hérisson, D., Brenet, M., Cliquet, D., Moncel, M.-H., Richter, J., Scott, B., Van Baelen, A., Di
- 1274 Modica, K., Loecker, D., Ashton, N., Bourguignon, L., Delagnes, A., Faivre, J.-P., Folgado-
- 1275 Lopez, M., Locht, J.-L., Pope, M., Raynal, J.-P., Roebroeks, W., Santagata, C., and Peer, P.:
- 1276 The emergence of the Middle Palaeolithic in north-western Europe and its southern fringes,
- 1277 Quaternary International, 411, https://doi.org/10.1016/j.quaint.2016.02.049, 2016.
- 1278 Hersbach, H., Bell, B., Berrisford, P., Hirahara, S., Horányi, A., Muñoz-Sabater, J., Nicolas, J.,
- Peubey, C., Radu, R., Schepers, D., Simmons, A., Soci, C., Abdalla, S., Abellan, X., Balsamo,
- 1280 G., Bechtold, P., Biavati, G., Bidlot, J., Bonavita, M., De Chiara, G., Dahlgren, P., Dee, D.,
- Diamantakis, M., Dragani, R., Flemming, J., Forbes, R., Fuentes, M., Geer, A., Haimberger,
- L., Healy, S., Hogan, R. J., Hólm, E., Janisková, M., Keeley, S., Laloyaux, P., Lopez, P., Lupu,
- 1283 C., Radnoti, G., de Rosnay, P., Rozum, I., Vamborg, F., Villaume, S., and Thépaut, J.-N.: The
- 1284 ERA5 global reanalysis, Quarterly Journal of the Royal Meteorological Society, 146, 1999-
- 1285 2049, https://doi.org/10.1002/qj.3803, 2020.
- 1286 Hodell, D. A., Channell, J. E. T., Curtis, J. H., Romero, O. E., and Röhl, U.: Onset of "Hudson
- 1287 Strait" Heinrich events in the eastern North Atlantic at the end of the middle Pleistocene
- 1288 transition (~640 ka)?, Paleoceanography, 23, 2008PA001591,
- 1289 https://doi.org/10.1029/2008PA001591, 2008.
- 1290 Hodell, D. A., Crowhurst, S. J., Lourens, L., Margari, V., Nicolson, J., Rolfe, J. E., Skinner, L.
- 1291 C., Thomas, N. C., Tzedakis, P. C., Mleneck-Vautravers, M. J., and Wolff, E. W.: A 1.5-million-
- 1292 year record of orbital and millennial climate variability in the North Atlantic, Clim. Past, 19, 607–
- 1293 636, https://doi.org/10.5194/cp-19-607-2023, 2023.
- 1294 Hodge, E., Richards, D., Smart, P., Andreo, B., Hoffmann, D., Mattey, D., and González-
- 1295 Ramón, A.: Effective precipitation in southern Spain (~ 266 to 46 ka) based on a speleothem
- 1296 stable carbon isotope record, Quaternary Research, 69, 447–457,
- 1297 https://doi.org/10.1016/j.yqres.2008.02.013, 2008.
- 1298 Hublin, J. J.: The origin of Neandertals, Proceedings of the National Academy of Sciences,
- 1299 106, 16022–16027, https://doi.org/10.1073/pnas.0904119106, 2009.
- 1300 Jiménez-Amat, P. and Zahn, R.: Offset timing of climate oscillations during the last two glacial-
- interglacial transitions connected with large-scale freshwater perturbation, Paleoceanography,
- 1302 30, 768–788, https://doi.org/10.1002/2014PA002710, 2015.





- 1303 Jiménez-Moreno, G., Anderson, R. S., Ramos-Román, M. J., Camuera, J., Mesa-Fernández,
- 1304 J. M., García-Alix, A., Jiménez-Espejo, F. J., Carrión, J. S., and López-Avilés, A.: The
- 1305 Holocene Cedrus pollen record from Sierra Nevada (S Spain), a proxy for climate change in N
- 1306 Quaternary Science Reviews, 242, 106468,
- 1307 https://doi.org/10.1016/j.quascirev.2020.106468, 2020.
- Johnsen, S. J., Clausen, H. B., Dansgaard, W., Fuhrer, K., Gundestrup, N., Hammer, C. U., 1308
- Iversen, P., Jouzel, J., Stauffer, B., and Steffensen, J. P.: Irregular glacial interstadials 1309
- 1310 recorded in a new Greenland record, Nature, 359, 311-313, 1992.
- 1311 Jouzel, J., Masson-Delmotte, V., Cattani, O., Dreyfus, G., Falourd, S., Hoffmann, G., Minster,
- B., Nouet, J., Barnola, J. M., Chappellaz, J., Fischer, H., Gallet, J. C., Johnsen, S., 1312
- Leuenberger, M., Loulergue, L., Luethi, D., Oerter, H., Parrenin, F., Raisbeck, G., Raynaud, 1313
- 1314 D., Schilt, A., Schwander, J., Selmo, E., Souchez, R., Spahni, R., Stauffer, B., Steffensen, J.
- 1315 P., Stenni, B., Stocker, T. F., Tison, J. L., Werner, M., and Wolff, E. W.: Orbital and millennial
- Antarctic climate variability over the past 800,000 years, Science, 317, 793-796, 1316
- https://doi.org/10.1126/science.1141038, 2007. 1317
- Kallel, N., Duplessy, J.-C., Labeyrie, L., Fontugne, M., Paterne, M., and Montacer, M.: 1318
- Mediterranean pluvial periods and sapropel formation over the last 200 000 years, 1319
- 1320 Palaeogeography, Palaeoclimatology, Palaeoecology, 157, 45-58,
- https://doi.org/10.1016/S0031-0182(99)00149-2, 2000. 1321
- 1322 Kelly, M., Edwards, R., Cheng, H., Yuan, D., Cai, Y., Zhang, M., Lin, Y., and An, Z.: High
- 1323 resolution characterization of the Asian Monsoon between 146,000 and 99,000 years B.P. from
- 1324 Dongge Cave, China and global correlation of events surrounding Termination II,
- 1325 Palaeogeography, Palaeoclimatology, Palaeoecology, 236, 20-38,
- https://doi.org/10.1016/j.palaeo.2005.11.042, 2006. 1326
- 1327 Key, A. J. M., Jarić, I., and Roberts, D. L.: Modelling the end of the Acheulean at global and
- 1328 continental levels suggests widespread persistence into the Middle Palaeolithic, Humanit Soc
- Sci Commun, 8, 55, https://doi.org/10.1057/s41599-021-00735-8, 2021. 1329
- 1330 Koltai, G., Spötl, C., Shen, C.-C., Wu, C.-C., Rao, Z., Palcsu, L., Kele, S., Surányi, G., and
- 1331 Bárány-Kevei, I.: A penultimate glacial climate record from southern Hungary, Journal of
- Quaternary Science, 32, 946-956, https://doi.org/10.1002/jqs.2968, 2017. 1332
- Koutsodendris, A., Dakos, V., Fletcher, W. J., Knipping, M., Kotthoff, U., Milner, A. M., Müller, 1333
- U. C., Kaboth-Bahr, S., Kern, O. A., Kolb, L., Vakhrameeva, P., Wulf, S., Christanis, K., 1334
- 1335 Schmiedl, G., and Pross, J.: Atmospheric CO2 forcing on Mediterranean biomes during the
- 1336 past 500 kyrs, Nat Commun, 14, 1664, https://doi.org/10.1038/s41467-023-37388-x, 2023.
- Laskar, J., Robutel, P., Joutel, F., Gastineau, M., Correia, A. C. M., and Levrard, B.: A long-1337
- 1338 term numerical solution for the insolation quantities of the Earth, A&A, 428, 261-285,
- 1339 https://doi.org/10.1051/0004-6361:20041335, 2004.
- 1340 Lewis, S., Ashton, N., and Jacobi, R.: 9 - Testing Human Presence During the Last Interglacial
- 1341 (MIS 5e): A Review of the British Evidence, in: Developments in Quaternary Sciences, vol. 14,
- edited by: Ashton, N., Lewis, S. G., and Stringer, C., Elsevier, 125-164, 1342
- https://doi.org/10.1016/B978-0-444-53597-9.00009-1, 2011. 1343
- 1344 Li, T.-Y., Shen, C.-C., Huang, L.-J., Jiang, X.-Y., Yang, X.-L., Mii, H.-S., Lee, S.-Y., and Lo, L.:
- 1345 Stalagmite-inferred variability of the Asian summer monsoon during the penultimate glacial-
- 1346 interglacial period, Climate of the Past, 10, 1211-1219, https://doi.org/10.5194/cp-10-1211-
- 2014, 2014. 1347





- 1348 Lionello, P., Malanotte-Rizzoli, P., Boscolo, R., Alpert, P., Artale, V., Li, L., Luterbacher, J.,
- 1349 May, W., Trigo, R., Tsimplis, M., Ulbrich, U., and Xoplaki, E.: The Mediterranean climate: An
- overview of the main characteristics and issues, in: Developments in Earth and Environmental
- 1351 Sciences, vol. 4, edited by: Lionello, P., Malanotte-Rizzoli, P., and Boscolo, R., Elsevier, 1–26,
- 1352 https://doi.org/10.1016/S1571-9197(06)80003-0, 2006.
- 1353 Lisiecki, L. and Raymo, M.: Pliocene-Pleistocene stack of 57 globally distributed benthic 18O
- 1354 records., Paleoceanography, 20, https://doi.org/10.1029/2004PA001071, 2005.
- 1355 Lisiecki, L. E. and Stern, J. V.: Regional and global benthic δ18O stacks for the last glacial
- 1356 cycle, Paleoceanography, 31, 1368–1394, https://doi.org/10.1002/2016PA003002, 2016.
- Liu, J., Fang, N., Wang, F., Yang, F., and Ding, X.: Features of ice-rafted debris (IRD) at IODP
- 1358 site U1312 and their palaeoenvironmental implications during the last 2.6 Myr,
- 1359 Palaeogeography, Palaeoclimatology, Palaeoecology, 511, 364–378,
- 1360 https://doi.org/10.1016/j.palaeo.2018.09.002, 2018.
- de Lumley, M. A.: Les restes humains fossiles de la grotte du Lazaret. Généralités, approche
- démographique., in: Les restes humains fossiles de la grotte du Lazaret, Nice, Alpes-
- 1363 Maritimes. Des Homo erectus européens évolués en voie de néandertalisation, CNRS
- 1364 Editions, 217-220, 2018.
- 1365 Macklin, M. G., Fuller, I. C., Lewin, J., Maas, G. S., Passmore, D. G., Rose, J., Woodward, J.
- 1366 C., Black, S., Hamlin, R. H. B., and Rowan, J. S.: Correlation of fluvial sequences in the
- 1367 Mediterranean basin over the last 200 ka and their relationship to climate change, Quaternary
- 1368 Science Reviews, 21, 1633–1641, https://doi.org/10.1016/S0277-3791(01)00147-0, 2002.
- 1369 Magri, D. and Parra, I.: Late Quaternary western Mediterranean pollen records and African
- winds, Earth and Planetary Science Letters, 200, 401-408, https://doi.org/10.1016/S0012-
- 1371 821X(02)00619-2, 2002.
- 1372 Margari, V., Skinner, L. C., Tzedakis, P. C., Ganopolski, A., Vautravers, M., and Shackleton,
- 1373 N. J.: The nature of millennial-scale climate variability during the past two glacial periods,
- 1374 Nature Geosci, 3, 127–131, https://doi.org/10.1038/ngeo740, 2010.
- 1375 Margari, V., Skinner, L., Hodell, D., Martrat, B., Toucanne, S., Gibbard, P., Lunkka, J., and
- 1376 Tzedakis, C.: Land-ocean changes on orbital and millennial time scales and the penultimate
- 1377 glaciation, Geology, https://doi.org/10.1130/G35070.1, 2014.
- 1378 Martrat, B., Grimalt, J. O., Lopez-Martinez, C., Cacho, I., Sierro, F. J., Flores, J. A., Zahn, R.,
- 1379 Canals, M., Curtis, J. H., and Hodell, D. A.: Abrupt Temperature Changes in the Western
- 1380 Mediterranean over the Past 250,000 Years, Science, 306, 1762-1765,
- 1381 https://doi.org/10.1126/science.1101706, 2004.
- Martrat, B., Grimalt, J. O., Shackleton, N. J., de Abreu, L., Hutterli, M. A., and Stocker, T. F.:
- 1383 Four Climate Cycles of Recurring Deep and Surface Water Destabilizations on the Iberian
- 1384 Margin, Science, 317, 502–507, https://doi.org/10.1126/science.1139994, 2007.
- 1385 Martrat, B., Jimenez-Amat, P., Zahn, R., and Grimalt, J. O.: Similarities and dissimilarities
- 1386 between the last two deglaciations and interglaciations in the North Atlantic region, Quaternary
- 1387 Science Reviews, 99, 122–134, https://doi.org/10.1016/j.quascirev.2014.06.016, 2014.
- 1388 Masson-Delmotte, V., Stenni, B., Pol, K., Braconnot, P., Cattani, O., Falourd, S., Kageyama,
- 1389 M., Jouzel, J., Landais, A., Minster, B., Barnola, J. M., Chappellaz, J., Krinner, G., Johnsen,
- 1390 S., Röthlisberger, R., Hansen, J., Mikolajewicz, U., and Otto-Bliesner, B.: EPICA Dome C





- 1391 record of glacial and interglacial intensities, Quaternary Science Reviews, 29, 113-128,
- 1392 https://doi.org/10.1016/j.quascirev.2009.09.030, 2010.
- 1393 Mathias, C., Bourguignon, L., Brenet, M., Grégoire, S., and Moncel, M.-H.: Between new and
- inherited technical behaviours: a case study from the Early Middle Palaeolithic of Southern
- 1395 France, Archaeol Anthropol Sci, 12, 146, https://doi.org/10.1007/s12520-020-01114-1, 2020.
- 1396 Matthews, A., Affek, H. P., Ayalon, A., Vonhof, H. B., and Bar-Matthews, M.: Eastern
- 1397 Mediterranean climate change deduced from the Soreq Cave fluid inclusion stable isotopes
- and carbonate clumped isotopes record of the last 160 ka, Quaternary Science Reviews, 272,
- 1399 107223, https://doi.org/10.1016/j.quascirev.2021.107223, 2021.
- 1400 McCarron, A. P., Bigg, G. R., Brooks, H., Leng, M. J., Marshall, J. D., Ponomareva, V.,
- 1401 Portnyagin, M., Reimer, P. J., and Rogerson, M.: Northwest Pacific ice-rafted debris at 38°N
- 1402 reveals episodic ice-sheet change in late Quaternary Northeast Siberia, Earth and Planetary
- 1403 Science Letters, 553, 116650, https://doi.org/10.1016/j.epsl.2020.116650, 2021.
- 1404 McManus, J. F., Oppo, D. W., and Cullen, J. L.: A 0.5-Million-Year Record of Millennial-Scale
- 1405 Climate Variability in the North Atlantic, Science, 283, 971–975,
- 1406 https://doi.org/10.1126/science.283.5404.971, 1999.
- 1407 Melchionna, M., Di Febbraro, M., Carotenuto, F., Rook, L., Mondanaro, A., Castiglione, S.,
- 1408 Serio, C., Vero, V. A., Tesone, G., Piccolo, M., Diniz-Filho, J. A. F., and Raia, P.: Fragmentation
- 1409 of Neanderthals' pre-extinction distribution by climate change, Palaeogeography,
- 1410 Palaeoclimatology, Palaeoecology, 496, 146–154,
- 1411 https://doi.org/10.1016/j.palaeo.2018.01.031, 2018.
- Menviel, L., Capron, E., Govin, A., Dutton, A., Tarasov, L., Abe-Ouchi, A., Drysdale, R. N.,
- 1413 Gibbard, P. L., Gregoire, L., He, F., Ivanovic, R. F., Kageyama, M., Kawamura, K., Landais,
- 1414 A., Otto-Bliesner, B. L., Oyabu, I., Tzedakis, P. C., Wolff, E., and Zhang, X.: The penultimate
- deglaciation: protocol for Paleoclimate Modelling Intercomparison Project (PMIP) phase 4
- transient numerical simulations between 140 and 127 ka, version 1.0, Geoscientific
- 1417 Model Development, 12, 3649–3685, https://doi.org/10.5194/gmd-12-3649-2019, 2019.
- 1418 Michel, V., Delanghe-Sabatier, D., Bard, E., and Barroso Ruiz, C.: U-series, ESR and 14C
- studies of the fossil remains from the Mousterian levels of Zafarraya Cave (Spain): A revised
- 1420 chronology of Neandertal presence, Quaternary Geochronology, 15, 20-33,
- 1421 https://doi.org/10.1016/j.quageo.2012.12.008, 2013.
- Michel, V., Shen, G., Shen, C.-C., Duval, M., Woodhead, J., Chou, Y.-M., Hu, H.-M., Wu, C.-
- 1423 C., Kan, Y.-C., Yang, H., Yu, T.-L., Gallet, S., and Valensi, P.: Datations radioisotopiques (U-
- 1424 Th, U-Pb) et paléodosimétriques (ESR) des plus anciens sites préhistoriques des Alpes-
- Maritimes: la grotte du Vallonnet, le site de plein air de Terra Amata et la grotte du Lazaret, in:
- Bulletin du Musée d'Anthropologie préhistorique de Monaco, vol. 61, 65–80, 2022.
- Moncel, M., Vaissié, E., Marin, J., Fernandes, P., Abrunhosa, A., Hardy, B., Richard, M.,
- Torres, C., and Baena, J.: Early Middle Palaeolithic Occupations Dated to MIS 7 at the Abri du
- 1429 Maras (Ardèche, Southeast France), Journal of Paleolithic Archaeology, 2025.
- Moncel, M.-H., Ashton, N., Arzarello, M., Fontana, F., Lamotte, A., Scott, B., Muttillo, B.,
- Berruti, G., Nenzioni, G., Tuffreau, A., and Peretto, C.: Early Levallois core technology between
- Marine Isotope Stage 12 and 9 in Western Europe, Journal of Human Evolution, 139, 102735,
- 1433 https://doi.org/10.1016/j.jhevol.2019.102735, 2020.





- Moseley, G. E., Spötl, C., Cheng, H., Boch, R., Min, A., and Edwards, R. L.: Termination-II
- interstadial/stadial climate change recorded in two stalagmites from the north European Alps,
- 1436 Quaternary Science Reviews, 127, 229–239, https://doi.org/10.1016/j.quascirev.2015.07.012,
- 1437 2015
- 1438 Mudie, P.: Pollen distribution in recent marine sediments, eastern Canada, Canadian Journal
- of Earth Sciences, 19, 729–747, https://doi.org/10.1139/e82-062, 2011.
- 1440 Murat, A. (Ed.): Chapitre 41: Pliocene-pleistocene occurrence of sapropels in the western
- mediterranean sea and their relation to eastern mediterranean sapropels, in: Proceedings of
- the Ocean Drilling Program, 161 Scientific Results, vol. 161, Ocean Drilling Program,
- 1443 https://doi.org/10.2973/odp.proc.sr.161.1999, 1999.
- Nehme, C., Verheyden, S., Breitenbach, S. F. M., Gillikin, D. P., Verheyden, A., Cheng, H.,
- Edwards, R. L., Hellstrom, J., Noble, S. R., Farrant, A. R., Sahy, D., Goovaerts, T., Salem, G.,
- 1446 and Claeys, P.: Climate dynamics during the penultimate glacial period recorded in a
- speleothem from Kanaan Cave, Lebanon (central Levant), Quaternary Research, 90, 10–25,
- 1448 https://doi.org/10.1017/qua.2018.18, 2018.
- Nehme, C., Kluge, T., Verheyden, S., Nader, F., Charalambidou, I., Weissbach, T., Gucel, S.,
- 1450 Cheng, H., Edwards, R. L., Satterfield, L., Eiche, E., and Claeys, P.: Speleothem record from
- 1451 Pentadactylos cave (Cyprus): new insights into climatic variations during MIS 6 and MIS 5 in
- 1452 the Eastern Mediterranean, Quaternary Science Reviews, 250, 106663
- 1453 https://doi.org/10.1016/j.quascirev.2020.106663, 2020.
- Obrochta, S. P., Crowley, T. J., Channell, J. E. T., Hodell, D. A., Baker, P. A., Seki, A., and
- Yokoyama, Y.: Climate variability and ice-sheet dynamics during the last three glaciations,
- 1456 Earth and Planetary Science Letters, 406, 198-212,
- 1457 https://doi.org/10.1016/j.epsl.2014.09.004, 2014.
- Ochando, J., Carrión, J. S., Blasco, R., Fernández, S., Amorós, G., Munuera, M., Sañudo, P.,
- and Fernández Peris, J.: Silvicolous Neanderthals in the far West: the mid-Pleistocene
- palaeoecological sequence of Bolomor Cave (Valencia, Spain), Quaternary Science Reviews,
- 217, 247–267, https://doi.org/10.1016/j.quascirev.2019.03.015, 2019.
- 1462 Okuda, M., Yasuda, Y., and Setoguchi, T.: Middle to Late Pleistocene vegetation history and
- 1463 climatic changes at Lake Kopais, Southeast Greece, Boreas, 30, 73-82,
- 1464 https://doi.org/10.1111/j.1502-3885.2001.tb00990.x, 2001.
- Oppo, D. W., Keigwin, L. D., McManus, J. F., and Cullen, J. L.: Persistent suborbital climate
- variability in marine isotope stage 5 and termination II, Paleoceanography, 16, 280-292,
- 1467 https://doi.org/10.1029/2000PA000527, 2001.
- 1468 Oppo, D. W., McManus, J. F., and Cullen, J. L.: Evolution and demise of the Last Interglacial
- 1469 warmth in the subpolar North Atlantic, Quaternary Science Reviews, 25, 3268-3277,
- 1470 https://doi.org/10.1016/j.quascirev.2006.07.006, 2006.
- 1471 Ovsepyan, E. A. and Murdmaa, I. O.: Response of the bering sea to Heinrich Event 11, Lithol
- 1472 Miner Resour, 52, 442–446, https://doi.org/10.1134/S0024490217060062, 2017.
- 1473 Panera, J., Torres, T., Pérez-González, A., Ortiz, J. E., Rubio-Jara, S., and Val, D. U. del:
- 1474 Geocronología de la Terraza Compleja de Arganda en el valle del río Jarama (Madrid,
- 1475 España), Estudios Geológicos, 67, 495–504, https://doi.org/10.3989/egeol.40550.204, 2011.





- 1476 Panera, J., Rubio-Jara, S., Yravedra, J., Blain, H.-A., Sesé, C., and Pérez-González, A.:
- 1477 Manzanares Valley (Madrid, Spain): A good country for Proboscideans and Neanderthals,
- 1478 Quaternary International, 326–327, 329–343, https://doi.org/10.1016/j.quaint.2013.09.009,
- 1479 2014.
- 1480 Penaud, A., Eynaud, F., Turon, J. L., Zaragosi, S., Malaizé, B., Toucanne, S., and Bourillet, J.
- 1481 F.: What forced the collapse of European ice sheets during the last two glacial periods
- 1482 (150 ka B.P. and 18 ka cal B.P.)? Palynological evidence, Palaeogeography,
- 1483 Palaeoclimatology, Palaeoecology, 281, 66–78, https://doi.org/10.1016/j.palaeo.2009.07.012,
- 1484 2009.
- 1485 Penaud, A., Eynaud, F., Voelker, A. H. L., and Turon, J.-L.: Palaeohydrological changes over
- the last 50 ky in the central Gulf of Cadiz: complex forcing mechanisms mixing multi-scale
- 1487 processes, Biogeosciences, 13, 5357–5377, https://doi.org/10.5194/bg-13-5357-2016, 2016.
- 1488 Pereira, T., Cunha, P. P., Martins, A. A., Nora, D., Paixão, E., Figueiredo, O., Raposo, L.,
- Henriques, F., Caninas, J., Moura, D., and Bridgland, D. R.: Geoarchaeology of the Cobrinhos
- site (Vila Velha de Ródão, Portugal) a record of the earliest Mousterian in western Iberia,
- 1491 Journal of Archaeological Science: Reports, 24, 640-654,
- 1492 https://doi.org/10.1016/j.jasrep.2018.11.026, 2019.
- 1493 Pérez-Asensio, J. N., Frigola, J., Pena, L. D., Sierro, F. J., Reguera, M. I., Rodríguez-Tovar,
- 1494 F. J., Dorador, J., Asioli, A., Kuhlmann, J., Huhn, K., and Cacho, I.: Changes in western
- 1495 Mediterranean thermohaline circulation in association with a deglacial Organic Rich Layer
- 1496 formation in the Alboran Sea, Quaternary Science Reviews, 228, 106075,
- 1497 https://doi.org/10.1016/j.quascirev.2019.106075, 2020.
- 1498 Peyrégne, S., Slon, V., Mafessoni, F., de Filippo, C., Hajdinjak, M., Nagel, S., Nickel, B., Essel,
- 1499 E., Le Cabec, A., Wehrberger, K., Conard, N. J., Kind, C. J., Posth, C., Krause, J., Abrams,
- 1500 G., Bonjean, D., Di Modica, K., Toussaint, M., Kelso, J., Meyer, M., Pääbo, S., and Prüfer, K.:
- Nuclear DNA from two early Neandertals reveals 80,000 years of genetic continuity in Europe,
- 1502 Science Advances, 5, eaaw5873, https://doi.org/10.1126/sciadv.aaw5873, 2019.
- 1503 Pini, R., Ravazzi, C., and Donegana, M.: Pollen stratigraphy, vegetation and climate history of
- the last 215 ka in the Azzano Decimo core (plain of Friuli, north-eastern Italy), Quaternary
- 1505 Science Reviews, 28, 1268–1290, https://doi.org/10.1016/j.quascirev.2008.12.017, 2009.
- 1506 Pons, A. and Quézel, P.: A propos de la mise en place du climat méditerranéen, Compte-
- rendus de l'Académie des Sciences de Paris, Sciences de la terre et des planètes, 327, 755–
- 1508 760, 1998.
- 1509 Prasad, A. M., Iverson, L. R., and Liaw, A.: Newer Classification and Regression Tree
- 1510 Techniques: Bagging and Random Forests for Ecological Prediction, Ecosystems, 9, 181–199,
- 1511 https://doi.org/10.1007/s10021-005-0054-1, 2006.
- 1512 Quézel, P.: Réflexions sur l'évolution de la flore et de la végétation au Maghreb Méditerranéen,
- 1513 Ibis Press., Paris, 117 pp., 2000.
- 1514 Raia, P., Mondanaro, A., Melchionna, M., Di Febbraro, M., Diniz-Filho, J. A., Rangel, T.,
- 1515 Holden, P., Carotenuto, F., Edwards, N., Lima-Ribeiro, M., Profico, A., Maiorano, L.,
- 1516 Castiglione, S., Serio, C., and Rook, L.: Past Extinctions of Homo Species Coincided with
- 1517 Increased Vulnerability to Climatic Change, One Earth, 3, 480-490,
- 1518 https://doi.org/10.1016/j.oneear.2020.09.007, 2020.





- 1519 Railsback, L. B., Gibbard, P. L., Head, M. J., Voarintsoa, N. R. G., and Toucanne, S.: An
- optimized scheme of lettered marine isotope substages for the last 1.0 million years, and the
- 1521 climatostratigraphic nature of isotope stages and substages, Quaternary Science Reviews,
- 1522 111, 94–106, https://doi.org/10.1016/j.quascirev.2015.01.012, 2015.
- 1523 Rasmussen, S. O., Bigler, M., Blockley, S. P., Blunier, T., Buchardt, S. L., Clausen, H. B.,
- 1524 Cvijanovic, I., Dahl-Jensen, D., Johnsen, S. J., Fischer, H., Gkinis, V., Guillevic, M., Hoek, W.
- 1525 Z., Lowe, J. J., Pedro, J. B., Popp, T., Seierstad, I. K., Steffensen, J. P., Svensson, A. M.,
- 1526 Vallelonga, P., Vinther, B. M., Walker, M. J. C., Wheatley, J. J., and Winstrup, M.: A
- 1527 stratigraphic framework for abrupt climatic changes during the Last Glacial period based on
- 1528 three synchronized Greenland ice-core records: refining and extending the INTIMATE event
- 1529 stratigraphy, Quaternary Science Reviews, 106, 14–28,
- 1530 https://doi.org/10.1016/j.quascirev.2014.09.007, 2014.
- 1531 Rasmussen, T. L., Oppo, D. W., Thomsen, E., and Lehman, S. J.: Deep sea records from the
- 1532 southeast Labrador Sea: Ocean circulation changes and ice-rafting events during the last
- 1533 160,000 years, Paleoceanography, 18, https://doi.org/10.1029/2001PA000736, 2003.
- 1534 Regattieri, E., Zanchetta, G., Drysdale, R. N., Isola, I., Hellstrom, J. C., and Roncioni, A.: A
- 1535 continuous stable isotope record from the penultimate glacial maximum to the Last Interglacial
- 1536 (159–121 ka) from Tana Che Urla Cave (Apuan Alps, central Italy), Quaternary Research, 82,
- 1537 450, 2014.
- 1538 Renault, L., Oguz, T., Pascual, A., Vizoso, G., and Tintore, J.: Surface circulation in the Alborán
- 1539 Sea (western Mediterranean) inferred from remotely sensed data, J. Geophys. Res., 117,
- 2011JC007659, https://doi.org/10.1029/2011JC007659, 2012.
- 1541 Rios-Garaizar, J.: Early Middle Palaeolithic occupations at Ventalaperra cave (Cantabrian
- 1542 Region, Northern Iberian Peninsula), Journal of Lithic Studies, 3
- 1543 https://doi.org/10.2218/jls.v3i1.1287, 2016.
- Robles, M., Peyron, O., Ménot, G., Brugiapaglia, E., Wulf, S., Appelt, O., Blache, M., Vannière,
- 1545 B., Dugerdil, L., Paura, B., Ansanay-Alex, S., Cromartie, A., Charlet, L., Guédron, S., De
- 1546 Beaulieu, J.-L., and Joannin, S.: Climate changes during the Lateglacial in South Europe: new
- insights based on pollen and brGDGTs of Lake Matese in Italy, https://doi.org/10.5194/cp-
- 1548 2022-54, 2022.
- Robles, M., Peyron, O., Ménot, G., Elisabetta, B., Wulf, S., Appelt, O., Blache, M., Vannière,
- 1550 B., Dugerdil, L., Paura, B., Ansanay-Alex, S., Cromartie, A., Charlet, L., Guedron, S., de
- 1551 Beaulieu, jacques-L., and Joannin, S.: Climate changes during the Late Glacial in southern
- Europe: new insights based on pollen and brGDGTs of Lake Matese in Italy, 19, 493–515,
- 1553 https://doi.org/10.5194/cp-19-493-2023, 2023.
- Rogerson, M., Cacho, I., Jimenez-Espejo, F., Reguera, M. I., Sierro, F. J., Martinez-Ruiz, F.,
- 1555 Frigola, J., and Canals, M.: A dynamic explanation for the origin of the western Mediterranean
- 1556 organic-rich layers, Geochemistry, Geophysics, Geosystems, 9,
- 1557 https://doi.org/10.1029/2007GC001936, 2008.
- 1558 Rohling, E. J., Marino, G., and Grant, K. M.: Mediterranean climate and oceanography, and
- the periodic development of anoxic events (sapropels), Earth-Science Reviews, 143, 62–97,
- 1560 https://doi.org/10.1016/j.earscirev.2015.01.008, 2015.
- Rohling, E. J., Hibbert, F. D., Williams, F. H., Grant, K. M., Marino, G., Foster, G. L., Hennekam,
- 1562 R., de Lange, G. J., Roberts, A. P., Yu, J., Webster, J. M., and Yokoyama, Y.: Differences
- 1563 between the last two glacial maxima and implications for ice-sheet, δ18O, and sea-level





- 1564 reconstructions, Quaternary Science Reviews, 176, 1–28,
- 1565 https://doi.org/10.1016/j.quascirev.2017.09.009, 2017.
- 1566 Roucoux, K. H., de Abreu, L., Shackleton, N. J., and Tzedakis, P. C.: The response of NW
- 1567 Iberian vegetation to North Atlantic climate oscillations during the last 65kyr, Quaternary
- Science Reviews, 24, 1637–1653, https://doi.org/10.1016/j.quascirev.2004.08.022, 2005.
- 1569 Roucoux, K. H., Tzedakis, P. C., Lawson, I. T., and Margari, V.: Vegetation history of the
- 1570 penultimate glacial period (Marine isotope stage 6) at Ioannina, north-west Greece, Journal of
- 1571 Quaternary Science, 26, 616–626, https://doi.org/10.1002/jqs.1483, 2011.
- 1572 Rousseau, D.-D., Antoine, P., Boers, N., Lagroix, F., Ghil, M., Lomax, J., Fuchs, M., Debret,
- 1573 M., Christine, H., Moine, O., Gauthier, C., Jordanova, D., and Jordanova, N.: Dansgaard-
- 1574 Oeschger-like events of the penultimate climate cycle: the loess point of view, Climate of the
- 1575 Past, 16, 713–727, https://doi.org/10.5194/cp-16-713-2020, 2020.
- 1576 Rubio-Jara, S. and Panera, J.: Unravelling an essential archive for the European Pleistocene.
- 1577 The human occupation in the Manzanares valley (Madrid, Spain) throughout nearly 800,000
- 1578 years, Quaternary International, 520, 5-22, https://doi.org/10.1016/j.quaint.2018.08.007,
- 1579 2019.
- 1580 Rubio-Jara, S., Panera, J., Rodríguez-de-Tembleque, J., Santonja, M., and Pérez-González,
- 1581 A.: Large flake Acheulean in the middle of Tagus basin (Spain): Middle stretch of the river
- 1582 Tagus valley and lower stretches of the rivers Jarama and Manzanares valleys, Quaternary
- 1583 International, 411, 349–366, https://doi.org/10.1016/j.quaint.2015.12.023, 2016.
- 1584 Ruddiman, W. F.: Late Quaternary deposition of ice-rafted sand in the subpolar North Atlantic
- 1585 (lat 40° to 65°N), Geol Soc America Bull, 88, 1813, https://doi.org/10.1130/0016-
- 1586 7606(1977)88<1813:LQDOIS>2.0.CO;2, 1977.
- 1587 Sadori, L., Koutsodendris, A., Panagiotopoulos, K., Masi, A., Bertini, A., Combourieu-Nebout,
- 1588 N., Francke, A., Kouli, K., Joannin, S., Mercuri, A. M., Peyron, O., Torri, P., Wagner, B.,
- Zanchetta, G., Sinopoli, G., and Donders, T. H.: Pollen-based paleoenvironmental and
- 1590 paleoclimatic change at Lake Ohrid (south-eastern Europe) during the past 500 ka,
- 1591 Biogeosciences, 13, 1423–1437, https://doi.org/10.5194/bg-13-1423-2016, 2016.
- 1592 Salonen, J. S., Korpela, M., Williams, J. W., and Luoto, M.: Machine-learning based
- 1593 reconstructions of primary and secondary climate variables from North American and
- 1594 European fossil pollen data, Sci Rep, 9, 15805, https://doi.org/10.1038/s41598-019-52293-4,
- 1595 2019.
- 1596 Sánchez Goñi, M.: The climatic and environmental context of the Late Pleistocene, in:
- 1597 Updating Neanderthals. Understanding Behavioural Complexity in the Late Middle
- 1598 Palaeolithic., Elsevier/Academic Press, London, 165–169, https://doi.org/10.1016/B978-0-12-
- 1599 823498-3.00012-1, 2022.
- 1600 Sánchez Goñi, M. F.: Millennial-scale variability during the last glacial in vegetation records
- 1601 from Europe, Quaternary Science Reviews, 2010.
- Sánchez Goñi, M. S., I, C., J, T., J, G., F, S., J, P., J, G., and N, S.: Synchroneity between
- marine and terrestrial responses to millennial scale climatic variability during the last glacial
- period in the Mediterranean region, Climate Dynamics, 19, 95, 2002.
- 1605 Sánchez-Yustos, P.: El paleolítico antiguo en la cuenca del Duero. Instrumentos teóricos para
- la construcción de un modelo interpretativo de arqueología económica, 2009.





- 1607 Sánchez-Yustos, P. and Diez-Martín, F.: Dancing to the rhythms of the Pleistocene? Early
- 1608 Middle Paleolithic population dynamics in NW Iberia (Duero Basin and Cantabrian Region),
- 1609 Quaternary Science Reviews, 121, https://doi.org/10.1016/j.quascirev.2015.05.005, 2015.
- Santonja, M., Pérez-González, A., Panera, J., Rubio-Jara, S., and Méndez-Quintas, E.: The
- 1611 coexistence of Acheulean and Ancient Middle Palaeolithic techno-complexes in the Middle
- 1612 Pleistocene of the Iberian Peninsula, Quaternary International, 411, 367-377,
- 1613 https://doi.org/10.1016/j.quaint.2015.04.056, 2016.
- 1614 Santonja, M., Pérez-González, A., Baena, J., Panera, J., Méndez-Quintas, E., Uribelarrea, D.,
- 1615 Demuro, M., Arnold, L., Abrunhosa, A., and Rubio-Jara, S.: The Acheulean of the Upper
- 1616 Guadiana River Basin (Central Spain). Morphostratigraphic Context and Chronology, Front.
- 1617 Earth Sci., 10, https://doi.org/10.3389/feart.2022.912007, 2022.
- 1618 Sassoon, D., Lebreton, V., Combourieu-Nebout, N., Peyron, O., and Moncel, M.-H.:
- 1619 Palaeoenvironmental changes in the southwestern Mediterranean (ODP site 976, Alboran sea)
- during the MIS 12/11 transition and the MIS 11 interglacial and implications for hominin
- 1621 populations, Quaternary Science Reviews, 304, 108010,
- 1622 https://doi.org/10.1016/j.quascirev.2023.108010, 2023.
- 1623 Sassoon, D., Combourieu-Nebout, N., Peyron, O., Bertini, A., Toti, F., Lebreton, V., and
- Moncel, M.-H.: Pollen-based climatic reconstructions for the interglacial analogues of MIS 1
- 1625 (MIS 19, 11, and 5) in the southwestern Mediterranean: insights from ODP Site 976, Clim.
- 1626 Past, 21, 489–515, https://doi.org/10.5194/cp-21-489-2025, 2025.
- 1627 Savannah, M., Eelco, R., Timme, D., Katharine, G., Jörg, K., Gianluca, M., Francesca, S.,
- 1628 Francesca, C., Caterina, M., Anna, S., and Alessandra, N.: The "glacial" sapropel S6 (172 ka;
- 1629 MIS 6): A multiproxy approach to solve a Mediterranean "cold case," Palaeogeography,
- 1630 Palaeoclimatology, Palaeoecology, 650, 112384,
- 1631 https://doi.org/10.1016/j.palaeo.2024.112384, 2024.
- 1632 Scott, B.: Becoming Neanderthals: the earlier British middle palaeolithic, Oxbow books,
- 1633 Oxford, 2011.
- Shackleton, N. J.: Oxygen isotopes, ice volume and sea level, Quaternary Science Reviews,
- 1635 6, 183–190, https://doi.org/10.1016/0277-3791(87)90003-5, 1987.
- 1636 Shackleton, N. J., Hall, M. A., and Vincent, E.: Phase relationships between millennial-scale
- 1637 events 64,000–24,000 years ago, Paleoceanography, 15, 565–569,
- 1638 https://doi.org/10.1029/2000PA000513, 2000.
- Shackleton, N. J., Sánchez-Goñi, M. F., Pailler, D., and Lancelot, Y.: Marine Isotope Substage
- 1640 5e and the Eemian Interglacial, Global and Planetary Change, 36, 151-155,
- 1641 https://doi.org/10.1016/S0921-8181(02)00181-9, 2003.
- 1642 Shackleton, N. J., Fairbanks, R. G., Chiu, T., and Parrenin, F.: Absolute calibration of the
- Greenland time scale: implications for Antarctic time scales and for Δ14C, Quaternary Science
- 1644 Reviews, 23, 1513–1522, https://doi.org/10.1016/j.quascirev.2004.03.006, 2004.
- Shaw, A., Bates, M., Conneller, C., Gamble, C., Julien, M.-A., McNabb, J., Pope, M., and Scott,
- 1646 B.: The archaeology of persistent places: the Palaeolithic case ofLa Cotte de St Brelade,
- Jersey, Antiquity, 90, 1437–1453, https://doi.org/10.15184/aqy.2016.212, 2016.
- 1648 Shin, J., Nehrbass-Ahles, C., Grilli, R., Beeman, J., Parrenin, F., Teste, G., Landais, A.,
- Schmidely, L., Silva, L., Schmitt, J., Bereiter, B., Stocker, T., Fischer, H., and Chappellaz, J.:





- 1650 Millennial-scale atmospheric CO2 variations during the Marine Isotope Stage 6 period (190-
- 1651 135 ka), Climate of the Past, 16, https://doi.org/10.5194/cp-16-2203-2020, 2020.
- 1652 Sierro, F. J. and Andersen, N.: An exceptional record of millennial-scale climate variability in
- the southern Iberian Margin during MIS 6: Impact on the formation of sapropel S6, Quaternary
- 1654 Science Reviews, 286, 107527, https://doi.org/10.1016/j.quascirev.2022.107527, 2022.
- 1655 Sierro, F. J., Hodell, D. A., Andersen, N., Azibeiro, L. A., Jimenez-Espejo, F. J., Bahr, A.,
- 1656 Flores, J. A., Ausin, B., Rogerson, M., Lozano-Luz, R., Lebreiro, S. M., and Hernandez-Molina,
- 1657 F. J.: Mediterranean Overflow Over the Last 250 kyr: Freshwater Forcing From the Tropics to
- 1658 the Ice Sheets, Paleoceanography and Paleoclimatology, 35, e2020PA003931,
- 1659 https://doi.org/10.1029/2020PA003931, 2020.
- 1660 Silva, P. G., López-Recio, M., Tapias, F., Roquero, E., Morín, J., Rus, I., Carrasco-García, P.,
- 1661 Giner-Robles, J. L., Rodríguez-Pascua, M. A., and Pérez-López, R.: Stratigraphy of the Arriaga
- 1662 Palaeolithic sites. Implications for the geomorphological evolution recorded by thickened fluvial
- sequences within the Manzanares River valley (Madrid Neogene Basin, Central Spain),
- Geomorphology, 196, 138–161, https://doi.org/10.1016/j.geomorph.2012.10.019, 2013.
- 1665 Sinopoli, G., Peyron, O., Masi, A., Holtvoeth, J., Francke, A., Wagner, B., and Sadori, L.:
- 1666 Pollen-based temperature and precipitation changes in the Ohrid Basin (western Balkans)
- between 160 and 70 ka, Climate of the Past, 15, 53-71, https://doi.org/10.5194/cp-15-53-2019,
- 1668 2019.
- 1669 Skinner, L. C. and Shackleton, N. J.: Deconstructing Terminations I and II: revisiting the
- 1670 glacioeustatic paradigm based on deep-water temperature estimates, Quaternary Science
- 1671 Reviews, 25, 3312–3321, https://doi.org/10.1016/j.quascirev.2006.07.005, 2006.
- 1672 Stocker, T. F.: The Seesaw Effect, Science, 282, 61-62,
- 1673 https://doi.org/10.1126/science.282.5386.61, 1998.
- 1674 Sumner, G., Homar, V., and Ramis, C.: Precipitation seasonality in eastern and southern
- 1675 coastal Spain, Intl Journal of Climatology, 21, 219–247, https://doi.org/10.1002/joc.600, 2001.
- 1676 Svendsen, J. I., Alexanderson, H., Astakhov, V. I., Demidov, I., Dowdeswell, J. A., Funder, S.,
- 1677 Gataullin, V., Henriksen, M., Hjort, C., Houmark-Nielsen, M., Hubberten, H. W., Ingólfsson, Ó.,
- 1678 Jakobsson, M., Kjær, K. H., Larsen, E., Lokrantz, H., Lunkka, J. P., Lyså, A., Mangerud, J.,
- 1679 Matiouchkov, A., Murray, A., Möller, P., Niessen, F., Nikolskaya, O., Polyak, L., Saarnisto, M.,
- 1680 Siegert, C., Siegert, M. J., Spielhagen, R. F., and Stein, R.: Late Quaternary ice sheet history
- 1681 of northern Eurasia, Quaternary Science Reviews, 23, 1229-1271,
- 1682 https://doi.org/10.1016/j.quascirev.2003.12.008, 2004.
- Terradillos-Bernal, M., Demuro, M., Arnold, L. J., Jordá-Pardo, J. F., Clemente-Conte, I.,
- Benito-Calvo, A., and Díez Fernández-Lomana, J. C.: San Quirce (Palencia, Spain): new
- chronologies for the Lower to Middle Palaeolithic transition of south-west Europe, Journal of
- 1686 Quaternary Science, 38, 21–37, https://doi.org/10.1002/jgs.3460, 2023.
- 1687 Thabet, A. A., Maas, A. E., Lawson, G. L., and Tarrant, A. M.: Life cycle and early development
- 1688 of the thecosomatous pteropod Limacina retroversa in the Gulf of Maine, including the effect
- of elevated CO2 levels, Mar Biol, 162, 2235–2249, https://doi.org/10.1007/s00227-015-2754-
- 1690 1, 2015.
- 1691 Torres, C., Tapias, F., Demuro, M., Arnold, L., Arriolabengoa, M., Pérez, S., and Preysler, J.:
- 1692 The Acheulian site of Cantera Vieja (Madrid, Spain) and the Lower to Middle Palaeolithic
- transition in central Spain, https://doi.org/10.21203/rs.3.rs-4195503/v1, 2024.





- Toucanne, S., Zaragosi, S., Bourillet, J. F., Cremer, M., Eynaud, F., Van Vliet-Lanoë, B.,
- 1695 Penaud, A., Fontanier, C., Turon, J. L., Cortijo, E., and Gibbard, P. L.: Timing of massive
- 1696 'Fleuve Manche' discharges over the last 350 kyr: insights into the European ice-sheet
- oscillations and the European drainage network from MIS 10 to 2, Quaternary Science
- 1698 Reviews, 28, 1238–1256, https://doi.org/10.1016/j.quascirev.2009.01.006, 2009.
- 1699 Tzedakis, P. C., Hooghiemstra, H., and Pälike, H.: The last 1.35 million years at Tenaghi
- 1700 Philippon: revised chronostratigraphy and long-term vegetation trends, Quaternary Science
- 1701 Reviews, 25, 3416–3430, https://doi.org/10.1016/j.quascirev.2006.09.002, 2006.
- 1702 Tzedakis, P. C., Drysdale, R. N., Margari, V., Skinner, L. C., Menviel, L., Rhodes, R. H.,
- 1703 Taschetto, A. S., Hodell, D. A., Crowhurst, S. J., Hellstrom, J. C., Fallick, A. E., Grimalt, J. O.,
- 1704 McManus, J. F., Martrat, B., Mokeddem, Z., Parrenin, F., Regattieri, E., Roe, K., and
- 22 Zanchetta, G.: Enhanced climate instability in the North Atlantic and southern Europe during
- the Last Interglacial, Nat Commun, 9, 4235, https://doi.org/10.1038/s41467-018-06683-3,
- 1707 2018.
- 1708 Valensi, P., Aouraghe, H., Bailon, S., Cauche, D., Combier, J., Desclaux, E., Gagnepain, J.,
- 1709 Gaillard, C., Khatib, S., Lumley, H., Moigne, A.-M., Moncel, M.-H., and Notter, O.: Les
- peuplements préhistoriques dans le sud-est de la France à la fin du Pléistocène moyen : 400
- 1711 120 000 ans. Terra Amata, Orgnac 3, Baume Bonne, Lazaret. Cadre géochronologique et
- 1712 biostratigraphique, paléoenvironnements et évolution culturelle des derniers
- 1713 anténéandertaliens., 2005.
- 1714 Valensi, P., Michel, V., El Guennouni, K., and Liouville, M.: New data on human behavior from
- 1715 a 160,000 year old Acheulean occupation level at Lazaret cave, south-east France: An
- 1716 archaeozoological approach, Quaternary International, 316
- 1717 https://doi.org/10.1016/j.quaint.2013.10.034, 2013.
- 1718 Vidal-Matutano, P., Blasco, R., Sañudo, P., and Fernández Peris, J.: The Anthropogenic Use
- 1719 of Firewood During the European Middle Pleistocene: Charcoal Evidence from Levels XIII and
- 1720 XI of Bolomor Cave, Eastern Iberia (230–160 ka), Environmental Archaeology, 24, 269–284,
- 1721 https://doi.org/10.1080/14614103.2017.1406026, 2019.
- 1722 Wagner, B., Vogel, H., Francke, A., Friedrich, T., Donders, T., Lacey, J. H., Leng, M. J.,
- 1723 Regattieri, E., Sadori, L., Wilke, T., Zanchetta, G., Albrecht, C., Bertini, A., Combourieu-
- Nebout, N., Cvetkoska, A., Giaccio, B., Grazhdani, A., Hauffe, T., Holtvoeth, J., Joannin, S.,
- Jovanovska, E., Just, J., Kouli, K., Kousis, I., Koutsodendris, A., Krastel, S., Lagos, M., Leicher,
- 1726 N., Levkov, Z., Lindhorst, K., Masi, A., Melles, M., Mercuri, A. M., Nomade, S., Nowaczyk, N.,
- Panagiotopoulos, K., Peyron, O., Reed, J. M., Sagnotti, L., Sinopoli, G., Stelbrink, B., Sulpizio,
- 1728 R., Timmermann, A., Tofilovska, S., Torri, P., Wagner-Cremer, F., Wonik, T., and Zhang, X.:
- 1729 Mediterranean winter rainfall in phase with African monsoons during the past 1.36 million
- 1730 years, Nature, 573, 256–260, https://doi.org/10.1038/s41586-019-1529-0, 2019.
- Wainer, K., Genty, D., Blamart, D., Daëron, M., Bar-Matthews, M., Vonhof, H., Dublyansky, Y.,
- 1732 Pons-Branchu, E., Thomas, L., Calsteren, P., Quinif, Y., and Caillon, N.: Speleothem record
- of the last 180 ka in Villars cave (SW France): Investigation of a large δ 18O shift between
- 1734 MIS6 and MIS5, Quaternary Science Reviews QUATERNARY SCI REV, 30, 130-146,
- 1735 https://doi.org/10.1016/j.quascirev.2010.07.004, 2011.
- 1736 Wainer, K., Genty, D., Blamart, D., Bar-Matthews, M., Quinif, Y., and Plagnes, V.: Millennial
- 1737 climatic instability during penultimate glacial period recorded in a south-western France
- speleothem, Palaeogeography, Palaeoclimatology, Palaeoecology, 376, 122–131,
- 1739 https://doi.org/10.1016/j.palaeo.2013.02.026, 2013.





- Wang, Q., Wang, Y., Shao, Q., Liang, Y., Zhang, Z., and Kong, X.: Millennial-scale Asian
- monsoon variability during the late Marine Isotope Stage 6 from Hulu Cave, China, Quat. res.,
- 1742 90, 394–405, https://doi.org/10.1017/qua.2018.75, 2018.
- Wang, Y. J., Cheng, H., Edwards, R. L., An, Z. S., Wu, J. Y., Shen, C. C., and Dorale, J. A.: A
- 1744 high-resolution absolute-dated late Pleistocene Monsoon record from Hulu Cave, China,
- 1745 Science, 294, 2345–2348, https://doi.org/10.1126/science.1064618, 2001.
- 1746 Wenzel, S.: Neanderthal presence and behaviour in central and Northwestern Europe during
- 1747 MIS 5e, in: Developments in Quaternary Sciences, 173-193,
- 1748 https://doi.org/10.13140/2.1.2747.7442, 2007.
- White, M. J. and Pettitt, P. B.: The British Late Middle Palaeolithic: An Interpretative Synthesis
- 1750 of Neanderthal Occupation at the Northwestern Edge of the Pleistocene World, Journal of
- World Prehistory, 24, https://doi.org/10.1007/s10963-011-9043-9, 2011.
- 1752 Willis, K. J., Bennett, K. D., Walker, D., Gamble, C., Davies, W., Pettitt, P., and Richards, M.:
- 1753 Climate change and evolving human diversity in Europe during the last glacial, Philosophical
- 1754 Transactions of the Royal Society of London. Series B: Biological Sciences, 359, 243–254,
- 1755 https://doi.org/10.1098/rstb.2003.1396, 2004.
- 1756 Wilson, G. P., Frogley, M. R., Hughes, P. D., Roucoux, K. H., Margari, V., Jones, T. D., Leng,
- 1757 M. J., and Tzedakis, P. C.: Persistent millennial-scale climate variability in Southern Europe
- 1758 during Marine Isotope Stage 6, Quaternary Science Advances, 3, 100016,
- 1759 https://doi.org/10.1016/j.qsa.2020.100016, 2021.
- 1760 Xue, G., Cai, Y., Ma, L., Cheng, X., Cheng, H., Edwards, R. L., Li, D., and Tan, L.: A new
- speleothem record of the penultimate deglacial: Insights into spatial variability and centennial-
- scale instabilities of East Asian monsoon, Quaternary Science Reviews, 210, 113-124,
- 1763 https://doi.org/10.1016/j.quascirev.2019.02.023, 2019.
- 1764 Yaworsky, P. M., Nielsen, E. S., and Nielsen, T. K.: The Neanderthal niche space of Western
- 1765 Eurasia 145 ka to 30 ka ago, Sci Rep, 14, 7788, https://doi.org/10.1038/s41598-024-57490-4,
- 1766 2024.
- 1767 Yravedra, J., Rubio-Jara, S., Panera, J., Made, J. van der, and Pérez-González, A.:
- 1768 Neanderthal diet in fluvial environments at the end of the Middle Pleistocene/early Late
- 1769 Pleistocene of PRERESA site in the Manzanares Valley (Madrid, Spain), Quaternary
- 1770 International, 520, 72–83, https://doi.org/10.1016/j.quaint.2018.01.030, 2019.
- Zahn, R., Comas, M. C., and Klaus, A. (Eds.): Proceedings of the Ocean Drilling Program, 161
- 1772 Scientific Results, Ocean Drilling Program, https://doi.org/10.2973/odp.proc.sr.161.1999,
- 1773 1999.
- 1774 Zhang, J., Zolitschka, B., Hogrefe, I., Tsukamoto, S., Binot, F., and Frechen, M.: High-
- 1775 resolution luminescence-dated sediment record for the last two glacial-interglacial cycles from
- 1776 Rodderberg, Germany, Quaternary Geochronology, 82, 101535,
- 1777 https://doi.org/10.1016/j.quageo.2024.101535, 2024.
- 1778 Ziegler, M., Tuenter, E., and Lourens, L.: The precession phase of the boreal summer
- 1779 monsoon as viewed from the eastern Mediterranean (ODP Site 968), Quaternary Science
- 1780 Reviews, 29, https://doi.org/10.1016/j.quascirev.2010.03.011, 2010.

1781